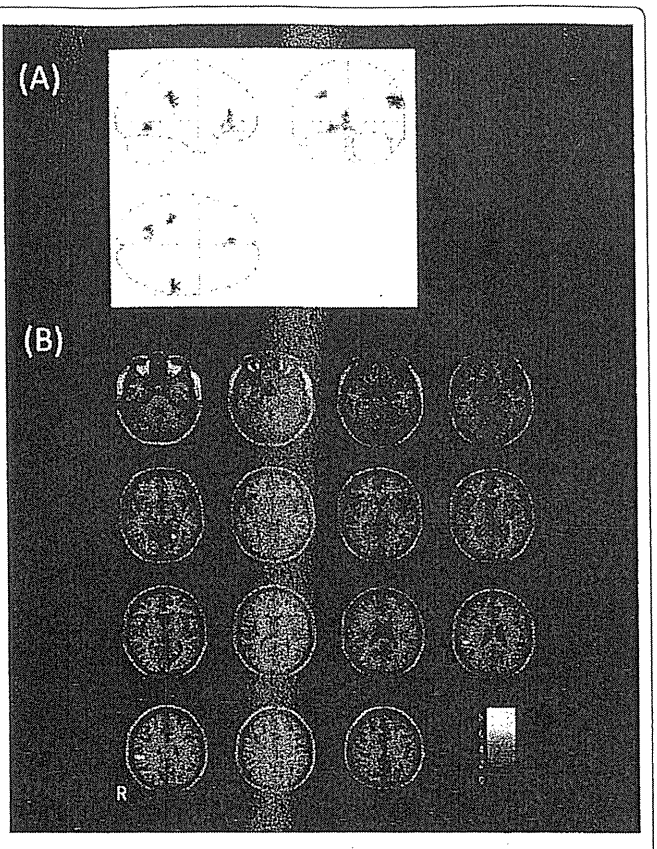

Figure 1 Results of voxel-based regression analysis between FA value and PM score. Regression analysis of FA value with a measure of prospective memory in DAI patients revealed four clusters, which are shown on (A) orthogonal projections (red arrowhead indicates the region of global maxima) and (B) axial view of MNI T1 template images. The clusters were observed in the right parietal lobes (Brodmann's area (BA) 40), left parahippocampal gyrus (BA19), left inferior parietal lobe (BA40), and left anterior cingulate gyrus (BA 32). The cluster located in the right inferior parietal lobe was excluded due to its location over the Sylvian fissure. Color bar indicates *T* value. (R = right hemisphere)

studies, except for anterior prefrontal cortex (aPFC), which has been suggested to be of central importance to PM by several researchers [6-10]. On post-hoc testing, the reduction of FA value in white matter close to aPFC was not significant compared with that in normal controls (data not shown). It is likely that an artifact originating from air in the frontal sinus masked the lesion in aPFC determined by FA value.

The present study is the first to evaluate the neuronal basis of PM using voxel-based regression analysis with FA maps in DAI subjects. An advantage of our methodology is that no experimental PM task was required; we could instead adopt the widely used clinical PM assessment battery. However, among the regions elicited by our method, we could not discriminate that attributable to core PM from that attributable to supportive function for PM.

Other limitations of our study include the following. First, we examined a relatively small number of subjects. Future studies with larger samples of patients are needed to augment the reliability of our findings. Second, DTI data were acquired with diffusion weighting encoded along only 6 independent orientations. To obtain more accurate tensor parameters, a larger number of gradient sampling orientations must be adopted in further studies. Third, the interval between injury and testing varied widely between 3 to 51 months. In a previous study, longitudinal decline of FA values was observed in brains subjected to trauma [29], suggesting that longitudinal changes in FA values may have affected our results. However, post-hoc examination revealed no significant decline in FA value with time from injury. Hence, FA values were not adjusted for time from injury. Despite these limitations, we believe that we were able to map the neuronal basis for PM performance in a daily life situation.

Conclusions

Using lesion-symptom analysis, we demonstrated that lesions in the left parahippocampal gyrus, left inferior parietal lobe, and/or left anterior cingulate resulted in PM failure. These structures may thus be included in the neuronal circuit of PM. Our findings reinforce those of previous activation studies with loading of experimental PM tasks.

Methods

Subjects

Fourteen DAI patients (males 13, female 1, age: range of 18-36, median 24) without focal brain injury participated in this study. They all meet Gennarelli's diagnostic criteria for DAI [30]. Diagnosis was confirmed by the

Table 2 Covariate regions between FA value and PM score

Cluster size	Peak *T* value	Peak Z score	Peak coordinates			Structure name	Nearest BA
			X	*Y*	*Z*		
128	7.0	4.3	-20	-60	-8	left parahippocampal gyrus	19
77	6.7	4.2	-30	-34	38	left inferior parietal lobe	40
108	6.3	4.1	-4	38	12	left anterior cingulate	32

$p < 0.001$(uncorrected), minimum cluster size = 50 voxels, voxel size 2 × 2 × 2 mm; *x*, *y*, and *z* values localize regions according to Montreal Neurological Institute stereotactic coordinates. (BA: Brodmann area)

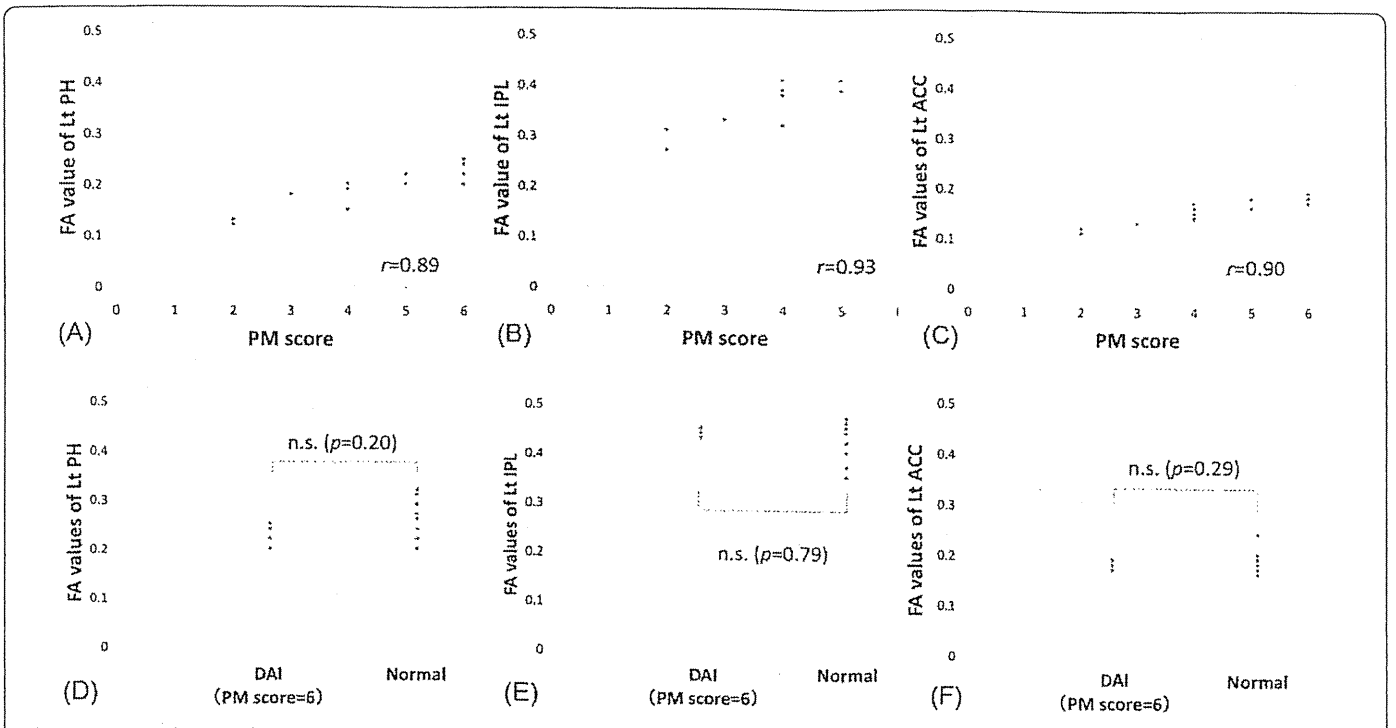

Figure 2 Correlations between FA value and PM score in each cluster and comparison with normal subjects. Significant correlations between FA value and PM score were found in (A) the left parahippocampal gyrus (r = 0.89), (B) left inferior parietal lobe (r = 0.93), and (C) left anterior cingulate (r = 0.90). FA values of DAI subjects with full PM score (score = 6) were preserved compared with those of normal volunteers in each cluster (D: left parahippocampal gyrus, E: left inferior parietal lobe, F: left anterior cingulate cortex). (Rt: right, Lt: left, FA: fractional anisotropy, PM: prospective memory, PH: parahippocampal gyrus, IPL: inferior parietal lobe, ACC: anterior cingulate cortex, n.s.: not significant).

presence of traumatic microbleeding on conventional T2*-weighted MR images [31]. Patients under 18 or over 40 years of age were excluded in order to prevent FA reduction related to lack of completion of development or aging [32]. All participants were right-handed. GCS at the time of injury was 3-7 (median 3, inter-quartile range 2), and all patients were classified as having severe TBI, according to the severity grading advocated by Narayan [33]. All participants with DAI were at least 3 months post-injury, with a mean time from injury of 16.3 (SD 16.1) months. Mean number of years of education was 13.6 (SD 2.4). The Wechsler Adult Intelligence Scale-III test was performed by all DAI subjects. Fourteen healthy age- and sex-matched volunteers without history of TBI, neurological disorder, or psychological disorder were participated. The mean number of years of education was 15.6 (SD 0.4). FA values of healthy participants were measured for the comparison of FA values in the extracted ROI analysis, between those of DAI patients. Informed consent for this study was given by the subject before the experiments. The experimental protocol was approved by the local ethics committee of Hiroshima Prefectural Rehabilitation Center.

PM assessment

Everyday memory performance was evaluated using standardized profile scores of the Rivermead Behavioural Memory Test (RBMT) in DAI patients [34]. PM failure was assessed using the following three sub-tests of RBMT. First, the belonging sub-test required the participants to ask for a personal belonging, which was taken from them at the beginning of the assessment, when the examiner indicated that the assessment had finished. Participants were also required to remember where the item was concealed. The second measure of PM was the appointment sub-test, in which participants were instructed to ask about a future appointment when a timer sounded. The final measure required the participants to deliver a message at a designated place while completing the RBMT route test. This sub-test had immediate and delayed (30 minutes later) components. In this study, we summed the standardized profile scores of these three sub-tests to obtain a measure of PM failure (scores range 0-6).

MR data acquisition

All MRIs were performed on a 1.5 T MR scanner (Siemens, 1.5 T Symphony, Erlangen, Germany) in all DAI and normal volunteers. Conventional axial T2-weighted and coronal fluid attenuated inversion recovery (FLAIR) images were obtained beforehand to rule out cerebral contusion or other lesions. Moreover, to confirm traumatic microbleeding, T2*-weighted transverse echo-planar images were obtained (data matrix, 256 × 256 with field of

view (FOV) 230 × 230 mm^2; 20 axial slices; repetition time (TR) 800 milliseconds; echo time (TE) 26 milliseconds; flip angle 20 degrees). DTI was performed using a single-shot spin echo planar imaging technique. Diffusion weighting was encoded along 6 independent orientations and the *b*-value was 1,000 s/mm^2, together with acquisition without diffusion weighting (b = 0). The diffusion-weighted imaging parameters were as follows: data matrix 256 × 256 with FOV 220 × 220 mm^2; 19 axial slices; 6 mm slice thickness; TR 4600 milliseconds; TE 137 milliseconds.

Data processing

In this study, DTI data processing was performed using DTI Studio software (Jiang H and Mori S, Johns Hopkins University, Kennedy Krieger Institute) to create FA maps [35]. For voxel-based statistical analysis, first the b = 0 images of all subjects were normalized to the standardized MNI T2 template of Statistical Parametric Mapping 2 (SPM2) software (Welcome Department of Imaging Neuroscience, London, UK) using an affine and nonlinear spatial normalization algorithm. Then the FA maps were normalized by applying the normalization parameters determined by normalization of the b = 0 images. The spatially normalized FA maps were then smoothed with a 6-mm isotropic Gaussian kernel to improve the signal-to-noise ratio, increase the validity of statistical inference, and improve normalization.

Statistics

Correlations between PM scores and clinical characteristics

Spearman's r correlation coefficients were calculated between PM scores and clinical parameters such as years of education, duration from onset, GCS at time of injury, and other neuropsychological scores.

Voxel-based regression analysis between PM score and FA value

Voxel-based regression analysis between FA value and PM score was performed using SPM2. In this study, statistical significance was defined by a voxel level threshold set at $p < 0.001$ (uncorrected for multiple comparisons) and clusters with a size larger than 50 contiguous voxels [36-39].

Cluster extracted statistics

Each cluster was automatically extracted using software (MarsBaR: http://marsbar.sourceforge.net/). Then, the location of each cluster was visually checked, and the adequacy of its anatomical location confirmed. Spearman's correlation coefficients were determined between the FA value of each cluster and PM score, and the times from injury, respectively. To evaluate whether the FA values were reserved in the patients whose PM performance were normal, we compared FA values in each cluster between DAI patients with full PM score and normal volunteers using the t-test.

These calculations were performed with SPSS Statistics for Windows version 17.0. P values less than 0.05 were considered significant unless otherwise indicated.

Additional material

Additional file 1: Results of voxel-based regression analysis between FA value and Trail making test-B. This figure demonstrates that the regions correlated with Trail making test-B (TMT-B) scores in the same DAI subjects. Thirteen patients were performed TMT-B, and the mean score was 140.2 (SD 50.6) seconds. There was no correlation between the measures of PM and TMT-B (r = -0.371, p = 0.213). Regression analysis of FA value with the score of TMT-B in DAI patients revealed three clusters, which are shown on (A) orthogonal projections (red arrowhead indicates the region of global maxima) and (B) coronal view of MNI T1 template images. The clusters were observed in the white matter of left pre-frontal lobes, right anterior cingulate, and left inferior parietal lobe. (C) Compared the cluster correlated with TMT-B (blue) with that correlated with PM (yellow), the cluster located in the left inferior parietal lobe was closed to each other. Color bar indicates T value. (R = right hemisphere)

Additional file 2: Covariate regions between FA value and Trail making test-B score. Regression analysis of FA value with the score of Trail Making Test-B in DAI patients revealed three clusters (x, y, and z values localize regions according to Montreal Neurological Institute stereotactic coordinates, BA = Brodmann area).

Acknowledgements

We thank the entire staff of the Hiroshima Higher Brain Function Center for assistance in subject recruitment and testing. This research was supported in part by grants from the General Insurance Association of Japan and from the Ministry of Health, Labour, and Welfare of Japan.

Author details

[1]Hiroshima Higher Brain Function Center, Hiroshima Prefectural Rehabilitation Center, 295-3, Taguchi, Saijo, Higashi-Hiroshima, Japan. [2]Department of Clinical Neuroscience & Therapeutics, Hiroshima University Graduate School of Biomedical Science, 1-2-3, Kasumi, Minami-ku, Hiroshima, Japan. [3]Department of Psychology, Fukuyama University, 958, Sanzo, Higashimura, Fukuyama, Japan. [4]Department of Communication Sciences and Disorders, Hiroshima Prefectural College of Health Sciences, 1-1, Gakuen-chou, Mihara, Hiroshima, Japan.

Authors' contributions

KK and MMar contributed to the design of this research. KK and HU performed the DTI data processing and statistical analysis. Neuropsychological assessment was performed by KS and HY. KK, TT, MMar, TOhs, and TOht participated in drafting of this manuscript. All authors read and approved the final manuscript and MMat has given final approval for publication of the final manuscript.

Competing interests

The authors declare that they have no competing interests.

Received: 12 February 2010 Accepted: 20 November 2010
Published: 20 November 2010

References

1. McDaniel MA, Einstein GO: Prospective memory: a new research enterprise. In *Prospective memory. An overview and synthesis of an emerging field.* Edited by: McDaniel MA, Einstein GO. California: Sage Publications; 2007:1-12.
2. Burgess PW, Veitch E, de Lacy Costello A, Shallice T: The cognitive and neuroanatomical correlates of multitasking. *Neuropsychologia* 2000, 38:848-863.

3. Kliegel M, Eschen A, Thöne-Otto AI: **Planning and realization of complex intentions in traumatic brain injury and normal aging.** *Brain Cogn* 2004, 56:43-54.
4. McDaniel MA, Einstein GO: **Cognitive neuroscience of prospective memory.** In *Prospective memory. An overview and synthesis of an emerging field.* Edited by: McDaniel MA, Einstein GO. California: Sage Publications; 2007:171-190.
5. Okuda J, Fujii T, Yamadori A, Kawashima R, Tsukiura T, Fukatsu R, Suzuki K, Ito M, Fukuda H: **Participation of the prefrontal cortices in prospective memory: evidence from a PET study in humans.** *Neurosci Lett* 1998, 253:127-130.
6. Okuda J, Fujii T, Ohtake H, Tsukiura T, Yamadori A, Frith CD, Burgess PW: **Differential involvement of regions of rostral prefrontal cortex (Brodmann area 10) in time- and event-based prospective memory.** *Int J Psychophysiol* 2007, 64:233-246.
7. Burgess PW, Quayle A, Frith CD: **Brain regions involved in prospective memory as determined by positron emission tomography.** *Neuropsychologia* 2001, 39:545-555.
8. Burgess PW, Scott SK, Frith CD: **The role of the rostral frontal cortex (area 10) in prospective memory: a lateral versus medial dissociation.** *Neuropsychologia* 2003, 41:906-918.
9. Simons JS, Schölvinck ML, Gilbert SJ, Frith CD, Burgess PW: **Differential components of prospective memory? Evidence from fMRI.** *Neuropsychologia* 2006, 44:1388-1397.
10. Reynolds JR, West R, Braver T: **Distinct neural circuits support transient and sustained processes in prospective memory and working memory.** *Cerebral Cortex* 2009, 19:1208-1221.
11. Adams JH, Graham DI, Murray LS, Scott G: **Diffuse axonal injury due to nonmissile head injury in humans: an analysis of 45 cases.** *Ann Neurol* 1982, 12:557-563.
12. Capruso DX, Levin HS: **Cognitive impairment following closed head injury.** *Neurol Clin* 1992, 10:879-893.
13. Evans RW: **The postconcussion syndrome and the sequelae of mild head injury.** *Neurol Clin* 1992, 10:815-847.
14. Levin HS, Mattis S, Ruff RM, Eisenberg HM, Marshall LF, Tabaddor K, High WM Jr, Frankowski RF: **Neurobehavioral outcome following minor head injury: a three-center study.** *J Neurosurg* 1987, 66:234-243.
15. Vakil E: **The effect of moderate to severe traumatic brain injury (TBI) on different aspects of memory: a selective review.** *J Clin Exp Neuropsychol* 2005, 27:977-1021.
16. Cockburn J: **Failure of prospective memory after acquired brain damage: preliminary investigation and suggestions for future directions [abstract].** *J Clin Exp Neuropsychol* 1996, 18:304-309.
17. Shum D, Valentine M, Cutmore T: **Performance of individuals with severe long-term traumatic brain injury on time-, event-, and activity-based prospective memory tasks.** *J Clin Exp Neuropsychol* 1999, 21:49-58.
18. Wieshmann UC, Symms MR, Clark CA, Lemieux L, Parker GJ, Shorvon SD: **Blunt-head trauma associated with widespread water-diffusion changes.** *Lancet* 1999, 353:1242-1243.
19. Nakayama N, Okumura A, Shinoda J, Yasokawa YT, Miwa K, Yoshimura SI, Iwama T: **Evidence for white matter disruption in traumatic brain injury without macroscopic lesions.** *J Neurol Neurosurg Psychiatry* 2006, 77:850-855.
20. Salmond CH, Menon DK, Chatfield DA, Williams GB, Pena A, Sahakian BJ, Pickard JD: **Diffusion tensor imaging in chronic head injury survivors: correlations with learning and memory indices.** *Neuroimage* 2006, 29:117-124.
21. Arfanakis K, Haughton VM, Carew JD, Rogers BP, Dempsey RJ, Meyerand ME: **Diffusion tensor MR imaging in diffuse axonal injury.** *AJNR Am J Neuroradiol* 2002, 23:794-802.
22. Huisman TA, Schwamm LH, Schaefer PW, Koroshetz WJ, Shetty-Alva N, Ozsunar Y, Wu O, Sorensen AG: **Diffusion tensor imaging as potential biomarker of white matter injury in diffuse axonal injury.** *AJNR Am J Neuroradiol* 2004, 25:370-376.
23. Mac Donald CL, Dikranian K, Song SK, Bayly PV, Holtzman DM, Brody DL: **Detection of traumatic axonal injury with diffusion tensor imaging in a mouse model of traumatic brain injury.** *Exp Neurol* 2007, 205:116-131.
24. Kraus MF, Susmaras T, Caughlin BP, Walker CJ, Sweeney JA, Little DM: **White matter integrity and cognition in chronic traumatic brain injury: a diffusion tensor imaging study.** *Brain* 2007, 130:2508-2519.
25. Kiehl KA, Laurens KR, Duty TL, Forster BB, Liddle PF: **Neural sources involved in auditory target detection and novelty processing: an event-related fMRI study.** *Psychophysiology* 2001, 38:133-142.
26. Asari T, Konishi S, Jimura K, Miyashita Y: **Multiple components of lateral posterior parietal activation associated with cognitive set shifting.** *Neuroimage* 2005, 26:694-702.
27. Moll J, Oliveria-Souza RD, Moll FT, Bramati IE, Andreiuolo PA: **The cerebral correlates of set-shifting; an fMRI study of the trail making test.** *Arq Neuropsiquiatr* 2002, 60:900-905.
28. West R, Krompinger J: **Neural correlates of prospective and retrospective memory.** *Neuropsychologia* 2005, 43:418-433.
29. Bendlin BB, Ries ML, Lazar M, Alexander AL, Dempsey RJ, Rowley HA, Sherman JE, Johnson SC: **Longitudinal changes in patients with traumatic brain injury assessed with diffusion-tensor and volumetric imaging.** *Neuroimage* 2008, 24:503-514.
30. Gennarelli TA: **Mechanism of brain injury.** *J Emerg Med* 1993, 11:5-11.
31. Scheid R, Preul C, Gruber O, Wiggins C, von Gramon Y: **Diffuse axonal injury associated with chronic traumatic brain injury: evidence from T2*-weighted gradient-echo imaging at 3T.** *AJNR Am J Neuroradiol* 2003, 24:1049-1056.
32. Grieve SM, Williams LM, Paul RH, Clark CR, Gordon E: **Cognitive aging, executive function, and fraction anisotropy: a diffusion tensor MR imaging study.** *AJNR Am J Neuroradiol* 2007, 28:226-235.
33. Narayan RK: **Emergency room management of the head-injured patient.** In *Textbook of head injury.* Edited by: Steven K, Gudeman. Philadelphia: WB Saunders Co; 1989:23-66.
34. Wilson BA, Cockburn J, Baddeley AD: **The Rivermead Behavioural Memory Test.** England: Thames Valley Test Co; 1985.
35. Jiang H, van Zijl PC, Kim J, Pearlson GD, Mori S: **Dtistudio: resource program for diffusion tensor computation and fiber bundle tracking.** *Comput Methods Programs Biomed* 2006, 81:106-116.
36. Xie S, Xiao JX, Gong GL, Zang YF, Wang YH, Wu HK, Jiang XX: **Voxel-based detection of white matter abnormalities in mild Alzheimer disease.** *Neurology* 2006, 66:1845-1849.
37. Schmithorst VJ, Wilke M, Dardzinski BJ, Holland SK: **Cognitive functions correlate with white matter architecture in a normal pediatric population: a diffusion tensor MRI study.** *Hum Brain Mapp* 2005, 26:139-147.
38. Ardekani BA, Nierenberg J, Hoptman MJ, Javitt DC, Lim KO: **MRI study of white matter diffusion anisotropy in schizophrenia.** *Neuroreport* 2003, 14:2025-2029.
39. Grasby PM, Frith CD, Friston KJ, Bench C, Frackowiak RS, Dolan RJ: **Functional mapping of brain areas implicated in auditory-verbal memory function.** *Brain* 1993, 116:1-20.

doi:10.1186/1471-2202-11-147
Cite this article as: Kondo *et al.*: The pathophysiology of prospective memory failure after diffuse axonal injury - Lesion-symptom analysis using diffusion tensor imaging. *BMC Neuroscience* 2010 11:147.

Submit your next manuscript to BioMed Central and take full advantage of:

- Convenient online submission
- Thorough peer review
- No space constraints or color figure charges
- Immediate publication on acceptance
- Inclusion in PubMed, CAS, Scopus and Google Scholar
- Research which is freely available for redistribution

Submit your manuscript at
www.biomedcentral.com/submit

BioMed Central

Downloaded from jnnp.bmj.com on June 3, 2010 - Published by group.bmj.com

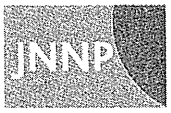

Bilateral hypogeusia in a patient with a unilateral paramedian thalamic infarction

Makoto Nakajima, Toshiho Ohtsuki and Kazuo Minematsu

J Neurol Neurosurg Psychiatry 2010 81: 700-701
doi: 10.1136/jnnp.2008.163485

Updated information and services can be found at:
http://jnnp.bmj.com/content/81/6/700.full.html

These include:

References This article cites 5 articles, 4 of which can be accessed free at:
http://jnnp.bmj.com/content/81/6/700.full.html#ref-list-1

Email alerting service Receive free email alerts when new articles cite this article. Sign up in the box at the top right corner of the online article.

Notes

To order reprints of this article go to:
http://jnnp.bmj.com/cgi/reprintform

To subscribe to *Journal of Neurology, Neurosurgery & Psychiatry* go to:
http://jnnp.bmj.com/subscriptions

Downloaded from jnnp.bmj.com on June 3, 2010 - Published by group.bmj.com

LETTERS

Bilateral hypogeusia in a patient with a unilateral paramedian thalamic infarction

Compared with other neurological deficits in patients with stroke, clinicians often overlook taste disorders, even though more than 30% of patients with acute stroke have taste disturbances.[1] Some authors have reported cases with bilateral taste disorders induced by a unilateral lesion in the brainstem, putamen, insular cortex or the parietal lobe. We present the first case of a bilateral taste disorder due to a unilateral paramedian thalamic infarction.

CASE REPORT

A 40s healthy person suddenly developed double vision on downward gaze and transient weakness of the right limbs. After 5 days, the patient became aware of paraesthesia and dullness of taste on both sides of the tongue. On the next day, the patient consulted our hospital and was admitted with a diagnosis of cerebral infarction.

The admission physical examination showed a blood pressure of 110/54 mm Hg, with a regular pulse of 60 beats/min. No abnormal sounds were heard on chest auscultation. On neurological examination, the patient was alert, and the visual fields were full. On downward gaze, the patient complained of double vision due to limitation of the left eye's downward movement. The pupils were isocoric, and both had prompt and complete light reflexes. The patient complained of paraesthesia and dullness of taste on both sides of the tongue. No abnormal findings were noted in the sensory and motor systems, including the deep tendon reflexes. Simple gait was stable and not ataxic.

The patient had a normal sinus rhythm; no atrial fibrillation was detected on either 12-lead electrocardiogram or 24 h Holter electrocardiogram monitoring. Transthoracic echocardiography was normal, and transesophageal echocardiography did not reveal an intracardiac right-to-left shunt or atherosclerotic lesions in the aortic arch. On electroencephalography, there were no epileptic discharges. Laboratory and haematological data were normal, including fibrinolytic and coagulation markers. Both lupus anticoagulant and antiphospholipid antibodies were negative. On brain diffusion-weighted MRI, there was evidence of an acute infarction in the paramedian region of the left thalamus (figure 1). Intra-arterial digital subtraction angiography (DSA) showed that the left posterior cerebral artery (PCA) had an irregular wall, and there was fenestration of the right PCA. On 3D-rotational DSA, an intimal flap was detected in the left PCA. Thus, a left perforating thalamic artery occluded by spontaneous dissection of the left PCA was diagnosed.

Oral aspirin 100 mg/day was prescribed on the day of admission. The patient's sense of taste was evaluated using the filter paper disc method of a commercial assay kit (Taste Disk, Sanwa Chemicals, Nagoya, Japan). This kit can be used to distinguish each fundamental taste (sweet, salty, sour and bitter) in the various regions corresponding to the appropriate nerves. A severe taste disturbance was seen on both sides 11 days postinfarction. In chorda tympani nerve area, hypogeusia was seen only in the left side, while severe hypogeusia was seen in both sides of glossopharyngeal nerve and greater petrosal nerve area. The taste disturbance partially improved by the 20th postinfarction day; the patient's subjective taste perceptions and paraesthesia of tongue had almost completely recovered by then. No ischaemic events occurred during the patient's hospital stay, and the patient's visual disturbance also improved gradually.

DISCUSSION

While hypogeusia caused by bilateral thalamic lesions was previously reported,[2] this is the first case of bilateral hypogeusia caused by a unilateral thalamic infarction. The lesion included the ventral posteromedial nucleus, which was found to have a strong association with the sense of taste in cat experiments.

In previous reports, unilateral supratentorial lesions tend to cause both bilateral and unilateral dysgeusia, while unilateral brainstem lesions under the midbrain or the pons tend to cause unilateral dysgeusia. This is probably due to the anatomy of the gustatory pathways. Gustatory pathways from the facial nerve, the glossopharyngeal nerve and vagus nerve connect to the ipsilateral solitary nucleus. Then, the tract ascends via the medial lemniscus to the contralateral parietal operculum (Brodmann's 43rd field), through the contralateral ventral posterior medial nucleus of the thalamus. However, controversy exists about this aspect.[3] The exact crossing area has also not yet been clarified.[4] Some authors suggest that the crossing occurs in the upper pons or midbrain.

In our case, a unilateral thalamic lesion caused bilateral taste dysfunction. We propose three possible mechanisms for this patient's dysgeusia. First, there may be a gustatory tract located both on the ipsilateral side and on the contralateral side of the gustatory receptor.[5] Second, the crossing site may be adjacent to the ventral posterior medial nucleus of the thalamus. Third, taste information from both sides of the tongue may be projected to the left insular cortex before ascending to the higher-order taste areas. However, the last hypothesis does not explain the cases reported with hemilateral dysgeusia due to supratentorial lesions on the left side.[1]

One of our patient's main symptoms was hypogeusia. Our patient was young and alert enough to complain of this subtle stroke symptom. The patient's dysgeusia improved over a short period of time, perhaps because of incomplete involvement of the unilateral gustatory tract. On the other hand, some authors have reported cases that lost weight over a period of years due to dysgeusia.

Our patient complained paraesthesia of tongue on admission. However, no objective trigeminal disorder was seen in sensory testing, and the symptoms decreased with improvement of taste disturbance. We speculated that severe taste disturbance might cause the subjective paraesthesia.

In conclusion, we report a case with left paramedian thalamic infarction who presented with bilateral hypogeusia. This case suggests the existence of a gustatory tract that ascends on the ipsilateral side from the solitary nucleus to the thalamus, or crosses near the level of the thalamus. To clarify the central gustatory pathway, patients' symptoms should be carefully elicited and the sense of taste examined, even in patients with stroke who do not complain of hypogeusia.

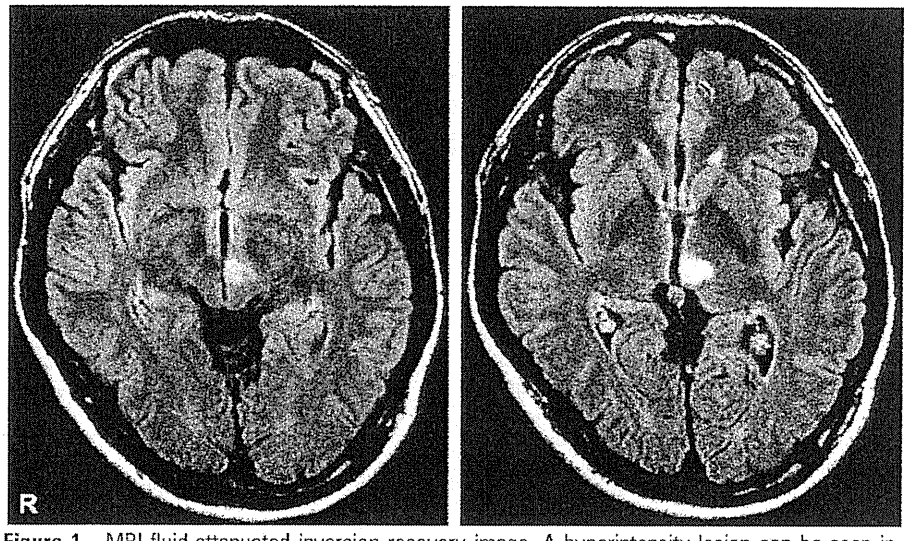

Figure 1 MRI fluid-attenuated inversion recovery image. A hyperintensity lesion can be seen in the paramedian lesion of the left thalamus.

Downloaded from jnnp.bmj.com on June 3, 2010 - Published by group.bmj.com

Makoto Nakajima, Toshiho Ohtsuki, Kazuo Minematsu

Cerebrovascular Division, Department of Medicine, National Cardiovascular Center, Osaka, Japan

Correspondence to Dr Makoto Nakajima, Department of Neurology, Stroke Center, Saiseikai Kumamoto Hospital, 5-3-1, Chikami, Kumamoto, 861–4193, Japan; nakazima@fc.kuh.kumamoto-u.ac.jp

Competing interests None.

Provenance and peer review Not commissioned; externally peer reviewed.

Received 21 September 2008
Revised 2 November 2008
Accepted 3 November 2008

J Neurol Neurosurg Psychiatry 2010;**81**:700–701. doi:10.1136/jnnp.2008.163485

REFERENCES

1. **Heckmann JG,** Stössel C, Lang CJ, *et al*. Taste disorders in acute stroke: a prospective observational study on taste disorders in 102 stroke patients. *Stroke* 2005;**36**:1690–4.
2. **Rousseaux M,** Muller P, Gahide I, *et al*. Disorders of smell, taste, and food intake in a patient with a dorsomedial thalamic infarct. *Stroke* 1996;**27**:2328–30.
3. **Heckmann JG,** Heckmann SM, Lang CJ, *et al*. Neurological aspects of taste disorders. *Arch Neurol* 2003;**60**:667–71.
4. **Landis BN,** Leuchter I, San Millán Ruíz D, *et al*. Transient hemiageusia in cerebrovascular lateral pontine lesions. *J Neurol Neurosurg Psychiatry* 2006;**77**:680–3.
5. **Shikama Y,** Kato T, Nagaoka U, *et al*. Localization of the gustatory pathway in the human midbrain. *Neurosci Lett* 1996;**218**:198–200.

Is tongue atrophy reversible in anti-MuSK myasthenia gravis? Six-year observation

Approximately 15% of myasthenia gravis (MC) patients do not have any detectable antiacetylcholine receptor (AChR) antibodies and are referred to as 'seronegative.' Of these, antibodies against muscle-specific tyrosine kinase (MuSK) are positive in 30–50%.[1 2] Tongue muscle atrophy is frequent in MuSK-positive MG.[3] The pathophysiology of muscle atrophy is unclear, and it has not yet been reported whether tongue muscle atrophy in MuSK-MG is reversible or not. We herein report a 6-year observation of tongue muscle atrophy with its MRI evaluation in a MuSK-MG patient.

In 2002, a 46-year-old woman was admitted with an 8-month history of progressive neck weakness, hoarseness and dysphagia. These symptoms did not fluctuate throughout the day. The patient had lost her body weight by 14 kg over 8 months. Neurological examination showed equivocal blepharoptosis on the right, prominent nasal voice and dysphagia, and mild atrophy of the tongue. There was moderate weakness in the neck muscles and mild weakness in the limbs. No fasciculations were observed. Tendon reflexes were active in all four limbs.

Serum anti-AChR antibodies were negative. The patient's percentage vital capacity (%VC) was decreased to 62%. An edrophonium test was negative. A repetitive nerve stimulation test showed no significant decremental responses in the nasalis, trapezius and abductor digiti minimi muscles. Axonal-stimulating single fibre electromyography (SFEMG) performed in the extensor digitorum communis (EDC) muscle showed slightly increased jitter (mean consecutive difference (MCD)=32 ms; normal <25 ms), and blocking was found in only in one of the 20 endplates examined. On electromyography, no resting potential was observed, and motor unit potentials were slightly polyphasic in the trapezius, first dorsal interosseous and tibialis anterior muscles.

The patient was tentatively diagnosed as having amyotrophic lateral sclerosis. The anti-MuSK antibody assay was not generally available in 2002. Seven months later, the patient developed CO_2 narcosis and underwent a tracheotomy, and mechanical ventilation was started.

In 2005, the patient was admitted again because of the lack of progression of limb weakness and amyotrophy for 3 years. Neurological examination revealed mild bilateral ptosis and weakness in the facial, bulbar, neck and respiratory muscles. Tongue muscle atrophy was substantially more prominent compared with findings in 2002.

Edrophonium test was negative, and repetitive nerve stimulation tests were also negative. On axonal-stimulating SFEMG, jitter was normal in the EDC (mean MCD=23 ms) but clearly increased in the frontalis muscle (mean MCD=128 ms with blocking in 65% of the endplates). Anti-MuSK antibody was found to be positive, with a titre of 8.8 nmol/l (normal <0.05 nmol/l). The diagnosis of MuSK-MG was made.

Plasmaphaeresis was performed four times. The patient's respiratory function rapidly improved, and 9 days after the initiation of plasmaphaeresis, mechanical ventilation was no longer required. Intravenous methylprednisolone (1000 mg/day for three consecutive days) was administered, followed by oral prednisolone 80 mg every other day. Her clinical improvement was dramatic; 5 weeks later, she had almost no difficulty in swallowing, or breathing, although tongue muscle atrophy and nasal voice remained.

The improved condition was maintained for 3 years after the start of treatment. Her tongue muscle atrophy was gradually improved, when prednisolone was discontinued in June 2007. In March 2008, the patient presented with only mild weakness of the facial and neck muscles. Daily living activities were not limited by the MG

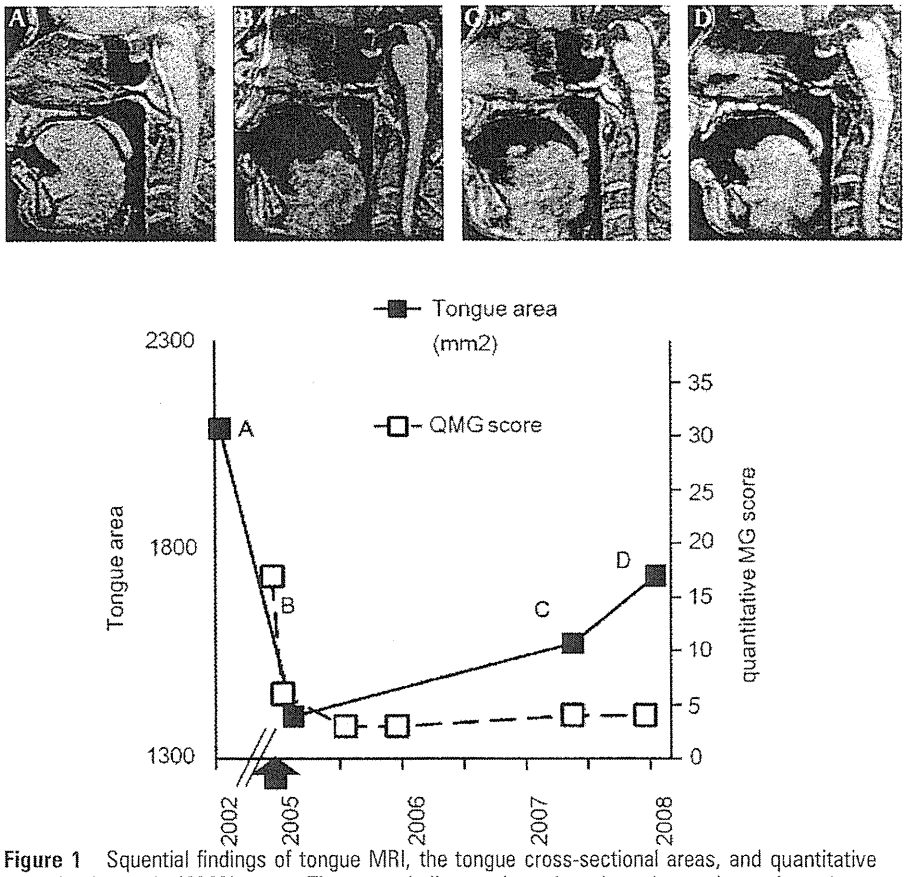

Figure 1 Squential findings of tongue MRI, the tongue cross-sectional areas, and quantitative myasthenia gravis (QMG) score. The arrow indicates the point when plasmaphaeresis and corticosteroid treatment were started. The dosage of predonisolone was reduced gradually and discontinued in June 2007.

Hypertension Research (2009) 32, 869–874
© 2009 The Japanese Society of Hypertension All rights reserved 0916-9636/09 $32.00
www.nature.com/hr

ORIGINAL ARTICLE

Association between central systolic blood pressure, white matter lesions in cerebral MRI and carotid atherosclerosis

Isha Shrestha[1], Tetsuya Takahashi[1], Eiichi Nomura[2], Toshiho Ohtsuki[1], Tomohiko Ohshita[1], Hiroki Ueno[1], Tatsuo Kohriyama[1] and Masayasu Matsumoto[1]

White matter hyperintensities (WMHs) observed on cerebral magnetic resonance images (MRIs) are associated with age and hypertension, suggesting a vascular mechanism of pathogenesis. Central systolic blood pressure (cSBP) correlates more closely with measures of cardiovascular disease risk than brachial pressure. We sought to determine whether cSBP correlates with WMHs and if cSBP is predictive of cerebrovascular disease. Radial applanation tonometric measurements for cSBP and augmentation index (AI) were carried out in unselected individuals undergoing carotid ultrasound. WMHs were assessed retrospectively using fluid-attenuated inversion recovery (FLAIR)-MRIs as periventricular (PVH) and deep white matter hyperintensities (DWMH), and they were rated using the Fazekas scale. A total of 179 patients, 94 (53%) men and 85 (47%) women, with a mean age of 66 ± 13 years were included in the study. On MRI, 17, 74, 67 and 21 patients had PVH grades 0, 1, 2 and 3, respectively. Forty-eight, 69, 49 and 13 had DWMH grades 0, 1, 2 and 3, respectively. In our study population, PVH correlated with age, brachial SBP, cSBP and AI (r=0.49, 0.28, 0.23; $P<0.002$ and r=0.13; $P<0.05$, respectively). DWMH also correlated with age, brachial SBP and cSBP (r=0.41, 0.30, 0.22; $P<0.003$, respectively), but not with AI. cSBP values were associated with PVH/DWMH grades 2 and 3, but brachial SBP correlated only with grade 3. Mean carotid intima–media thickness (common carotid arteries (CCA)-IMT) was 0.68 ± 0.13 mm. CCA-IMT and plaque score (PS) correlated with PVH/DWMH. Multivariate regression analysis showed cSBP, age and PS to be independently associated with PVH and DWMH. Correlation of cSBP with PVH and DWMH was independent of PS. Central SBP correlated with PVH and DWMH in FLAIR-MRIs and can better predict WMHs than brachial SBP in earlier stages.
Hypertension Research (2009) **32**, 869–874; doi:10.1038/hr.2009.121; published online 31 July 2009

Keywords: arterial stiffness; atherosclerosis; carotid artery intima–media thickness; central systolic blood pressure; cerebral white matter hyperintensities

INTRODUCTION

White matter lesions (WMLs) are frequently observed on cerebral magnetic resonance images (MRIs) of elderly patients without apparent neurological symptoms.[1] These WMLs appear as hyperintense areas in T2-weighted and fluid-attenuated inversion recovery (FLAIR) MRIs and as isointense areas in T1-weighted MRIs. Their presence correlates with gait disturbances,[2] cognitive impairment, dementia[3] and mood disorders.[4] Epidemiological studies have shown that age, hypertension and diabetes, the principal risk factors of cerebrovascular disease (CVD), are associated with white matter hyperintensities (WMHs). This association is suggestive of a vascular mechanism in WMH pathogenesis.[1,5–7] The presence of WMHs is an independent risk factor for stroke.[8] Pathological studies have shown definite structural vascular abnormalities associated with WMHs, strengthening the argument that WMHs have a vascular etiology,[9,10] and thus suggesting that WMHs are associated with atherosclerotic changes in small vessels.

Ultrasonographic findings of increased atherosclerotic plaques and carotid artery intima–media thickness (IMT) are also regarded as the subclinical markers of early atherosclerosis. The presence of these markers is associated with non-modifiable and modifiable risk factors and with the subsequent risk of new or recurrent stroke and myocardial infarction.[11–13] Conversely, studies show that the presence of atherosclerosis is predictive of WMHs.[5,14] The severity of IMT and the presence of plaques in the carotid arteries are also predictive of periventricular WMLs.[15]

Recently, several non-invasive parameters have been introduced to assess vascular stiffness. Central systolic blood pressure (cSBP) and augmentation index (AI) are parameters obtained non-invasively from central arterial waveforms through radial arterial pulse wave analysis

[1]Department of Clinical Neuroscience and Therapeutics, Hiroshima University, Hiroshima, Japan and [2]Department of Neurology, Suiseikai Kajikawa Hospital, Hiroshima, Japan
Correspondence: Dr T Takahashi, Department of Clinical Neuroscience and Therapeutics, Hiroshima University Graduate School of Biomedical Sciences, 1-2-3 Kasumi, Minami-ku, Hiroshima 734-8551, Japan.
E-mail: tetakaha@mac.com
Received 30 April 2009; revised 10 June 2009; accepted 16 June 2009; published online 31 July 2009

(PWA).[16–18] AI and cSBP are closely related to several risk factors for atherosclerosis and future cardiovascular events.[18–21]

In this study, we investigated the relationship between WMHs and enhanced arterial stiffness and sought to determine whether cSBP correlates with WMHs and can serve as a predictor of CVD. We obtained cSBP and AI through PWA and recorded WMHs as detected by FLAIR-MRIs. We also investigated the association of cSBP with carotid atherosclerosis.

METHODS

Study population

Study participants were recruited from unselected consecutive cases attending the carotid ultrasonography clinic for clinically indicated ultrasonographic examination of the extracranial carotid arteries. The study population encompassed a wide range of age groups and underlying diseases including patients with CVD, coronary artery disease, and other neurological and systemic problems. Also included were patients undergoing carotid ultrasonography for preoperative screening. Exclusion criteria included inability to perform the tonometric PWA as in patients with atrial fibrillation, chronic renal failure with patent arteriovenous fistulas in bilateral wrists for hemodialysis, aortitis with impalpable peripheral pulses, inability to obtain MRIs (as patients with pacemakers and other implants), inability to obtain a good carotid sonograph, and inability to obtain informed consent from the patient. Informed consent was obtained from all participants before they were enrolled in the study.

Ultrasound evaluation

The common carotid arteries (CCA) were evaluated using high-resolution B-mode duplex ultrasonography with a 7.5-MHz linear type probe (Aplio, Toshiba Medicals, Tokyo, Japan). Bilateral optimal visualization of the carotid artery was performed with the patients lying in the supine position with their necks slightly hyperextended. We obtained the mean value of maximal IMT measured in the distal CCA far wall (CCA-IMT), the 10-mm section of the artery proximal to the starting point of the carotid bulb. Measurements were taken from the best longitudinal images obtained after multiple visualizations. Plaques in the accessible segments of the CCA as well as the internal carotid artery were described in terms of plaque number and plaque score (PS). Plaques are defined as IMT $\geqslant$ 1.1 mm. Plaque number is the total number of plaques recorded in the CCA-internal carotid artery segments bilaterally. PS is the sum of the heights of all the plaques present bilaterally.[22,23]

Pulse wave analysis

Measurements were taken in a quiet, temperature-controlled room with the patient sitting comfortably on a bed after completing the carotid ultrasonography. Applanation tonometry of the radial artery was performed in the left wrist using the commercially available automated applanation tonometry system (HEM-9000AI, Omron Healthcare, Kyoto, Japan). The built-in software in the Omron system was used to obtain the following measurements: AI, brachial SBP, cSBP, diastolic blood pressure (DBP) and pulse pressure. The validity of the device has already been established.[24]

MRI data acquisition

Participants' MRI findings were obtained retrospectively from the hospital's electronic data bank. We used the most recent images (within the past 6 months, except for three cases where images as old as 10 months were included). The patients were examined on the 1.5 T MRI unit (SIGNA, GE Medical Systems, Fairfield, CT, USA). The WMHs in MRIs were classified into periventricular hyperintensities (PVH) and deep white matter hyperintensities (DWMH). PVH and DWMH were defined as showing high intensity in FLAIR-MRIs and low intensity in T1-weighted MRIs. PVH includes WMHs in contact with the ventricular wall, and DWMH includes the WMHs situated in the deep white matter and separated from the ventricular wall by a strip of normal-appearing white matter. The severity of PVH and DWMH was rated visually on axial-FLAIR images using the Fazekas scale[25] to assign grades 0–3. A single person performed visual ratings of PVH and DWMH in a blinded manner.

Risk factors

Data regarding the patients' risk factors for atherosclerosis, such as hypertension, diabetes mellitus, dyslipidemia, history of stroke or transient ischemic attack, ischemic heart disease or coronary artery disease, and smoking habits were obtained from hospital records. Risk factors were defined as follows: hypertension: SBP $\geqslant$ 140 mm Hg and/or DBP $\geqslant$ 90 mm Hg or using antihypertensive medication; diabetes mellitus: fasting blood glucose $\geqslant$ 7.0 mmol l^{-1} or using oral hypoglycemic agents or insulin; dyslipidemia: low-density lipoprotein-cholesterol $\geqslant$ 3.6 mmol l^{-1} or using lipid-lowering agents; smoking was defined as 'current smokers' or 'nonsmokers.'

Statistical analysis

Statistical analyses were performed using the Statistical Package for the Social Sciences (version 11.5. for Windows, SPSS Inc., Chicago, IL, USA). Data are expressed as mean ± s.d. or %, unless stated otherwise. Pearson's and Spearman's correlation coefficients were used for continuous and ordinal variables, respectively. Comparison of the variables between groups was carried out using the χ^2-test for categorical variables and analysis of variance and post hoc tests (Tukey HSD) for continuous variables. Univariate correlation analyses were used to assess the relationships between variables of interest. Multivariate

Table 1 Characteristics of patients with different grades of PVH and DWMH

		MRI-PVH grades				*MRI-DWMH grades*			
Characteristics	*Total*	*0*	*1*	*2*	*3*	*0*	*1*	*2*	*3*
N	179	17	74	67	21	48	69	49	13
Male (%)	94 (52.5)	10 (58.8)	39 (52.7)	33 (49.3)	11 (52.4)	30 (62.5)	32 (46.4)	26 (53.1)	5 (38.5)
Age (years)	66 ± 13	43 ± 14	65 ± 11	71 ± 10	71 ± 9	57 ± 16	67 ± 11	72 ± 10	71 ± 11
cSBP (mm Hg)	137 ± 18	123 ± 19	137 ± 24	141 ± 22	152 ± 28	129 ± 20	140 ± 21	141 ± 27	161 ± 30
SBP (mm Hg)	131 ± 12	122 ± 16	131 ± 21	135 ± 21	148 ± 24	125 ± 16	134 ± 20	137 ± 24	153 ± 26
AI (%)	83 ± 17	74 ± 15	82 ± 15	85 ± 18	85 ± 17	78 ± 17	85 ± 16	82 ± 17	91 ± 11
HR (beats min^{-1})	73 ± 13	75 ± 15	72 ± 12	74 ± 14	71 ± 11	75 ± 14	72 ± 11	75 ± 15	67 ± 9
DBP (mm Hg)	78 ± 13	75 ± 14	77 ± 11	79 ± 13	77 ± 14	75 ± 12	78 ± 12	79 ± 12	74 ± 15
PP (mm Hg)	56 ± 18	48 ± 15	54 ± 17	57 ± 17	71 ± 24	50 ± 14	55 ± 16	58 ± 20	78 ± 25
CCA-IMT (mm)	0.68 ± 0.13	0.62 ± 0.14	0.77 ± 0.15	0.83 ± 0.17	0.91 ± 0.35	0.72 ± 0.15	0.79 ± 0.17	0.83 ± 0.15	0.98 ± 0.41
Plaque score	3.37 ± 3.57	1.12 ± 2.50	2.0 ± 2.26	2.93 ± 2.51	3.57 ± 3.52	1.59 ± 2.62	2.51 ± 2.23	2.84 ± 2.57	3.69 ± 3.74

Abbreviations: AI, augmentation index; CCA-IMT, common carotid artery intima–media thickness; cSBP, central systolic blood pressure; DBP, diastolic blood pressure; DWMH, deep white matter hyperintensities; HR, heart rate; *N*, number; PVH, periventricular hyperintensities; SBP, brachial systolic blood pressure; PP, pulse pressure; PS, plaque score.
Data are presented as mean ± s.d. or as the number (%) of patients.

linear regression analysis was carried out to check the independent relationships of cSBP with WMHs. All *P*-values <0.05 were considered statistically significant.

RESULTS

A total of 179 patients were included in the study. Of the total participants, 94 (52.5%) were males. The mean ± s.d. age of the participants was 66 ± 13 years (median, 68 years). Clinical characteristics for each grade of PVH and DWMH are shown in Table 1. Of the total patients, 88 had a history of stroke and 14 had a history of coronary artery disease or ischemic heart disease. Among the stroke patients, 12.1% had transient ischemic attacks, 4.0% had hemorrhagic strokes and 83.9% had ischemic strokes. With respect to subtypes of ischemic stroke, 34.3% had large artery atherosclerosis, 12.1% had cardioembolic events, 29.3% had small artery occlusion, 2.0% had strokes of other determined cause, and 6.1% had strokes of undetermined cause according to the TOAST classification.

Table 2 shows the diagnosis and risk factors of the study participants. The number of patients with PVH grades 0, 1, 2 and 3 was 17, 74, 67 and 21, respectively. Similarly, the number of patients with DWMH grades 0, 1, 2 and 3 was 48, 69, 49 and 13, respectively. Of the total patients, 41 (22.9%) were taking antihypertensive medications. PVH and DWMH correlated with the diagnosis of hypertension ($r=-0.36$, $P<0.0001$ and $r=-0.36$, $P<0.0001$, respectively) and past history of CVD ($r=-0.22$, $P<0.003$ and $r=-0.16$, $P<0.036$), but they did not show any association with diabetes mellitus, dyslipidemia, past coronary artery disease or smoking habits. Investigation of the association between the MRI findings and cSBP in men and women separately showed that women had a stronger association than men.

Univariate analysis revealed that cSBP is correlated with brachial SBP and also moderately with AI (Figure 1). CCA-IMT showed a significant positive correlation with cSBP, as well as AI, but the association was weaker with AI compared with cSBP (Figure 1).

Table 2 Clinical characteristics of the study participants

	Men (n=94)	*Women (n=85)*	*P-value*
Age (years)	66	65	<0.001
Hypertension (%)	56.4	45.9	NS
Antihypertension therapy	22.3	24.7	NS
Calcium channel blocker	5.6	8.9	
Angiotensin receptor blocker	6.7	3.9	
ACE inhibitor	2.2	5.0	
Diuretics/β-blockers/others	6.1	3.4	
Diabetes mellitus (%)	34.5	24.7	<0.002
Dyslipidemia (%)	29.8	44.7	<0.0001
Smoking habits (%)	55.3	14.1	0.0002
History of CVD (%)	50.0	47.1	NS
History of CAD (%)	4.3	9.4	<0.001
Parkinsonism (%)	10.6	14.1	NS
Dementias (%)	3.2	9.4	0.042
Other neurological diseases (%)[a]	18.1	23.5	NS
Other systemic diseases (%)[b]	16.0	11.8	NS

Abbreviations: ACE, angiotensin-converting enzyme; CAD, coronary artery disease; CVD, cerebrovascular disease; IHD, ischemic heart disease; NS, not significant; *n*, number; TIA, transient ischemic attack.
Values are the mean or frequency. *P*-values refer to un-paired *t*-test for continuous variables and χ^2-analysis for categorical variables.
[a]Includes cases with vertigo, neuropathies, seizure disorders, migraine and so on.
[b]Includes patients with renal and hepatic disorders, various cancers, those undergoing carotid ultrasonography for preoperative screening.

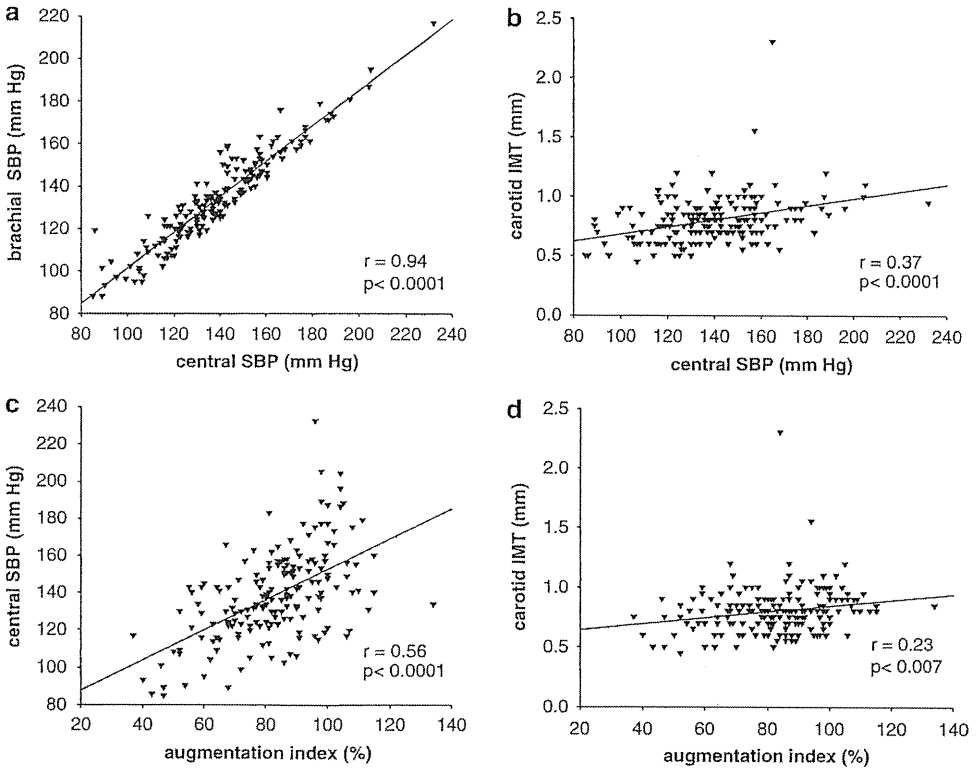

Figure 1 Univariate analyses among the parameters: scatter plots showing the relationships between brachial systolic blood pressure (SBP) and central SBP ($y=17.64+0.89x$) (**a**); carotid intima–media thickness (IMT) and central SBP ($y=0.38+0.00x$) (**b**); central SBP and augmentation index (AI) ($y=71.76+0.81x$) (**c**); and carotid IMT and AI ($y=0.59+0.00x$) (**d**).

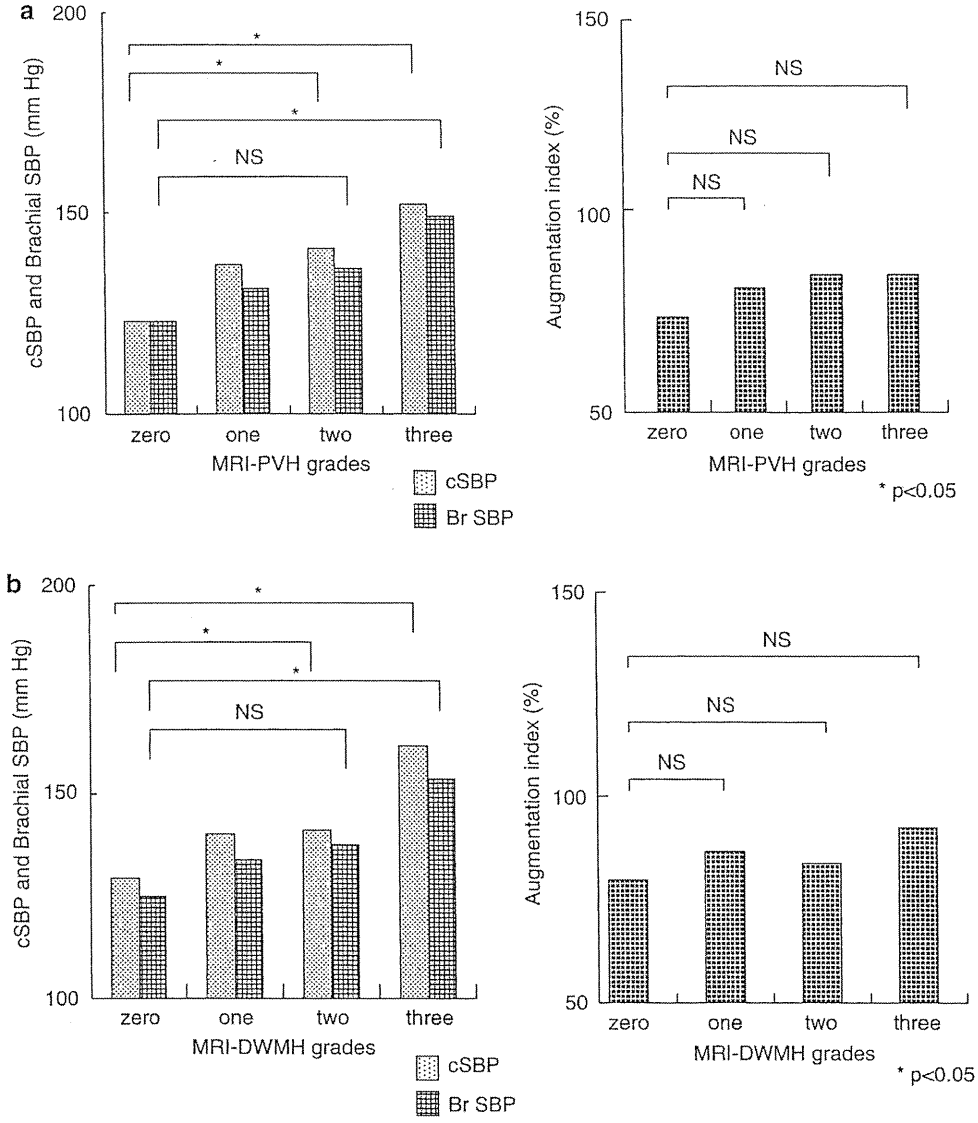

Figure 2 Central systolic blood pressure (cSBP) values showed a significant association with the periventricular hyperintensities (PVH) and deep white matter hyperintensities (DWMH) grades 2 and 3, but brachial SBP had a significant association with only the extreme grades (grade 3) of both PVH and DWMH (panels a and b). The grades of both PVH and DWMH did not correlate with the augmentation index (AI). Analysis of variance, *post hoc* test (Tukey HSD). *$P<0.05$; NS, not significant.

In the correlation analysis, the presence of PVH showed positive correlations with age ($r=0.49$, $P<0.0001$), SBP ($r=0.28$, $P<0.0001$) and cSBP ($r=0.23$, $P<0.002$). DWMH also showed associations with age ($r=0.41$, $P<0.0001$), SBP ($r=0.30$, $P<0.001$) and cSBP ($r=0.22$, $P<0.003$). PVH was correlated with AI ($r=0.13$, $P<0.05$), but DWMH was not. The presence of PVH was positively correlated with CCA-IMT, PS and plaque number but not with DBP or pulse pressure. Positive correlation was also seen between DWMH and CCA-IMT, PS, plaque number and pulse pressure but not with DBP.

The cSBP values in the PVH grades 0, 1, 2 and 3 were 123 ± 19, 137 ± 24, 141 ± 22 and 152 ± 28 mm Hg, respectively. The cSBP values in the DWMH grades 0, 1, 2 and 3 were 129 ± 20, 140 ± 21, 141 ± 24 and 161 ± 30 mm Hg, respectively. When the relationships between the increasing PVH grades and parameters of PWA were investigated, cSBP showed a significant positive correlation with PVH grades, whereas AI was not correlated (Figure 2a). DWMH grades also showed significant correlations with cSBP but not with AI (Figure 2b). The differences in the cSBP values in PVH and DWMH grades 0 and 3 as well as 0 and 2 were significant, but for the brachial SBP, the differences were significant only for grades 0 and 3 (Figures 2a and b).

The mean CCA-IMT in the total study sample was 0.68 ± 0.13 mm. CCA-IMT increased along with increases in PVH and DWMH grades. Similarly, PS also increased with the increase in PVH and DWMH grades (Table 1).

The results of multivariate linear regression analysis in stepwise manner, with PVH and DWMH grades as dependent variables, are shown in Table 3. In model 1, we adjusted for age, male sex, AI, CCA-IMT and PS. In model 2, we also adjusted for cSBP. We found that cSBP, but not AI, was independently related to PVH and DWMH. Age and PS also showed independent relationships with PVH and DWMH.

Patients with PVH and DWMH grades 0 or 1 (PVH I and DWMH I) and grades 2 and 3 (PVH II and DWMH II) were stratified into two groups on the basis of their PS grades (Figure 3). PS grades were

divided into PS I (no or mild PS that is, PS < 5) and PS II (moderate-to-severe PS that is, PS ≥ 5) groups. *T*-test analysis of the differences in the mean cSBP values between the two groups of PVH and DWMH against PS I and II groups showed significant differences in the PS I groups.

DISCUSSION

The main finding of this study is that cSBP is positively correlated with the presence of PVH and DWMH in FLAIR-MRIs in an unselected sample. Our results show that the cSBP values are more closely associated than the brachial SBP with PVH and DWMH grades. Although we found that cSBP also tended to correlate with the atherosclerotic changes in the carotid arteries, the association between cSBP and WMHs was independent of the atherosclerotic changes.

The cSBP values showed significant association not only with high-grade (grade three) lesions but also with the lower grade PVH and DWMH lesions. By contrast, brachial SBP is only significantly associated with these lesions for the extreme grades but not for the lower grades. Though brachial SBP has been and still is an important risk factor, we can suggest from our data that cSBP might be a better predictive indicator, especially to predict the PVH/DWMH lesions in their earlier stages. Further studies with much larger sample sizes are needed to validate the results. To the best of our knowledge, our study is the first to examine the relationships of cSBP with PVH and DWMH.

Table 3 Stepwise linear regression analysis of white matter hyperintensities with other parameters

	PVH presence				*DWMH presence*			
	Model 1		*Model 2*		*Model 1*		*Model 2*	
Correlate	*β*	P	*β*	P	*β*	P	*β*	P
Age	0.49	<0.001	0.42	<0.001	0.40	<0.001	0.31	<0.001
Gender (male sex)	0.07	NS	0.09	NS	0.11	NS	0.15	NS
AI	0.02	NS	0.03	NS	0.03	NS	0.05	NS
CCA-IMT	0.15	NS	0.12	NS	0.16	NS	0.10	NS
Plaque score	0.17	0.02	0.17	0.02	0.22	0.004	0.21	0.006
cSBP			0.14	0.03			0.19	0.008

Abbreviations: AI, augmentation index; cSBP, central systolic blood pressure; CCA-IMT, common carotid artery intima–media thickness; DWMH, deep white matter hyperintensities; NS, not significant; PVH, periventricular hyperintensities.
Results of correlation analysis of PVH presence and DWMH presence to parameters of radial wave analysis; cSBP and AI; and carotid atherosclerosis. Model 1 adjusted for age, gender (male sex), AI, CCA-IMT or plaque score. Model 2 adjusted for variables in Model 1, cSBP.
The strength of correlation is expressed by the regression coefficients β.

White matter lesions are frequently observed on cerebral MRIs of elderly patients without apparent neurological symptoms.[1] These WMLs appear as hyperintense areas in T2-weighted and FLAIR-MRIs and as isointense areas in T1-weighted MRIs. They reportedly correlate with gait disturbances,[2] cognitive impairment, dementia[3] and mood disorders.[4] These WMLs are likely to result from ischemic injury to the brain.[26] Exposure of vessels to high pressure results in impairment of cerebral autoregulation[27] or microvascular structural damage,[28] and these are potential mechanisms that may lead to cerebral WMHs. This would represent the cerebral manifestation of hypertensive target organ damage. In a population-based study, Roman *et al.*[29] showed that central pressures more accurately reflect the loading conditions on the cerebral vasculature than brachial pressures do. There are also data suggesting that central pressure and indices correlate more closely with the measures of cardiovascular risk than brachial pressure and that they can independently predict future cardiovascular events.[17,30–32] Furthermore, the results of a large-scale ASCOT-CAFÉ study show that brachial blood pressure is not always a good surrogate for the effects of blood pressure-lowering drugs on arterial hemodynamics, emphasizing the importance of central blood pressure measurements over traditional peripheral blood pressure measurements.[33]

Differing from most of the other studies[20,34,35] that focus on the association between WMHs and arterial stiffness with brachial artery pulse wave velocity parameters, this study examined the relationships of WMHs with cSBP and AI. Increased brachial artery pulse wave velocity is reported to be closely associated with the appearance of PVH in elderly populations[35] and also with the risk of small vessel disease in hypertensive elderly persons.[34] Although the measurement techniques are different, our results support similar findings that stiffness of arteries, in our case cSBP, is associated with WMLs.

In our study, we established a good association between the MRI-WMHs and cSBP, but no such association existed with AI. The different relationships of AI and cSBP with WMHs in our study could be explained by assuming that these two measurements provide different information about arterial structure and function. As age, height, DBP[36] and heart rate[37] are known determinants of AI, AI does not reflect arterial stiffness alone. We suppose, for this very reason, that the association between AI and WMHs was weaker in this study.

In this study, we uniquely investigated the MRI-WMHs in unselected patients, unlike earlier studies in which within risk-factor groups were included. Similar to earlier studies,[1,2] our study also showed that age is independently associated with both PVH and DWMH. Females had a stronger association between the MRI findings and cSBP. In addition, cerebral WMHs are associated with carotid

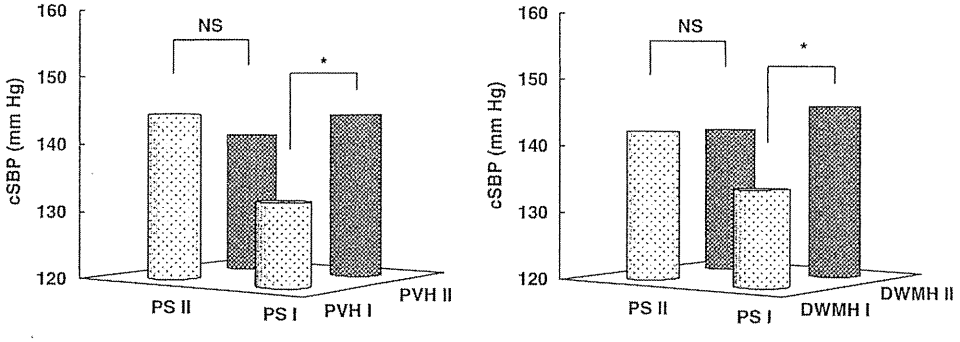

Figure 3 Central systolic blood pressure (cSBP) in patients with periventricular hyperintensities (PVH) grades 0 or 1 (PVH I) and PVH grades 2 or 3 (PVH II) and in patients with deep white matter hyperintensities (DWMH) grades 0 or 1 (DWMH I) and DWMH grades 2 or 3 (DWMH II), stratified into two groups according to the plaque score (PS) grades, PS I (PS < 5) and PS II (PS ≥ 5). *P*-values refer to *t*-tests. **P* < 0.05; NS, not significant.

IMT and PS, as suggested by this study, and also supported by earlier studies.[5,13,15] The presence of aortic atherosclerosis at middle age is predictive for the development of WMLs later in life.[14] But, with further analysis, only PS was independently associated with both PVH and DWMH. The results show that differences in cSBP values between the higher and lower grades of PVH/DWMH were significantly independent of PSs.

In summary, we found that cSBP and brachial SBP show varying degrees of association with PVH and DWMH detected in MRIs. cSBP is more strongly correlated with both PVH and DWMH. We believe that cSBP shows a stronger association with different grades of MRI lesions and systemic atherosclerotic changes. For economical and technical reasons, the measurement of cSBP using radial applanation tonometry could serve as a practical and reliable tool to predict cerebral WMLs and assess atherosclerotic changes.

This study had some limitations. First, the relatively small sample size limits our statistical power. In addition, we cannot establish a causal relationship between the parameters because of the cross-sectional study design. Larger longitudinal studies capable of supporting the relationship between cSBP and the increased risk of CVD found in this study are needed.

In conclusion, this study shows that increased cSBP is closely related to cerebral WMHs in unselected patients. Thus, cSBP might not only serve as a better predictor of CVD but also be used in the regular clinical setting.

ACKNOWLEDGEMENTS

We thank Ms Akime Enomura (Department of Clinical Neuroscience and Therapeutics, Hiroshima University) for conducting all the carotid ultrasonographies in this study

Funding: The study was partially funded by the Ministry of Education, Culture, Sports, Science and Technology of Japan.

Financial support: The applanation tonometric device (HEM-9000AI, Omron Healthcare Co. Ltd.) used in the study was kindly provided by Omron Healthcare Co. Ltd., Kyoto, Japan.

1 de Leeuw FE, de Groot JC, Achten E, Oudkerk M, Ramos LM, Heijboer R, Hofman A, Jolles J, van Gijn J, Breteler MMB. Prevalence of cerebral white matter lesions in elderly people: a population based magnetic resonance imaging study. The Rotterdam Scan Study. *J Neurol Neurosurg Psychiatry* 2001; **70**: 9–14.
2 Baezner H, Blahak C, Poggesi A, Pantoni L, Inzitari D, Chabriat H, Erkinjuntti T, Fazekas F, Ferro JM, Langhorne P, O'Brien J, Scheltens P, Visser MC, Wahlund LO, Waldemar G, Wallin A, Hennerici MG. Association of gait and balance disorders with age-related white matter changes: the LADIS study. *Neurology* 2008; **70**: 935–942.
3 Holland CM, Smith EE, Csapo I, Gurol ME, Brylka DA, Killiany RJ, Blacker D, Albert MS, Guttmann CR, Greenberg SM. Spatial distribution of white-matter hyperintensities in Alzheimer disease, cerebral amyloid angiopathy, and healthy aging. *Stroke* 2008; **39**: 1127–1133.
4 Takahashi K, Oshima A, Ida I, Kumano H, Yuuki N, Fukuda M, Amanuma M, Endo K, Mikuni M. Relationship between age at onset and magnetic resonance image-defined hyperintensities in mood disorders. *J Psychiatr Res* 2008; **42**: 443–450.
5 Pico F, Dufouil C, Lévy C, Besançon V, de Kersaint-Gilly A, Bonithon-Kopp C, Ducimetiere P, Tzourio C, Alperovitch A. Longitudinal study of carotid atherosclerosis and white matter hyperintensities: the EVA-MRI cohort. *Cerebrovasc Dis* 2002; **14**: 109–115.
6 de Leeuw FE, de Groot JC, Oudkerk M, Witteman JC, Hofman A, van Gijn J, Breteler MMB. Hypertension and cerebral white matter lesions in a prospective cohort study. *Brain* 2002; **125**: 765–772.
7 Vermeer SE, Hollander M, van Dijk EJ, Hofman A, Koudstaal PJ, Breteler B, Rotterdam Scan Study. Silent brain infarcts and white matter lesions increase stroke risk in the general population: the Rotterdam Scan Study. *Stroke* 2003; **34**: 1126–1129.
8 Barber R, Scheltens P, Gholkar A, Ballard C, McKeith I, Ince P, Perry R, O'Brien J. White matter lesions on magnetic resonance imaging in dementia with Lewy bodies, Alzheimer's disease, vascular dementia, and normal aging. *J Neurol Neurosurg Psychiatry* 1999; **67**: 66–72.
9 Young VG, Halliday GM, Kril JJ. Neuropathologic correlates of white matter hyperintensities. *Neurology* 2008; **71**: 804–811.
10 Jagust WJ, Zheng L, Harvey DJ, Mack WJ, Vinters HV, Weiner MW, Ellis WG, Zarow C, Mungas D, Reed BR, Kramer JH, Schuff N, DeCarli C, Chui HC. Neuropathological basis of magnetic resonance images in aging and dementia. *Ann Neurol* 2008; **63**: 72–80.
11 Ebrahim S, Papacosta O, Whincup P, Wannamethee G, Walker M, Nicolaides AN, Dhanjil S, Griffin M, Belcaro G, Rumley A, Lowe GD. Carotid plaque, intima media thickness, cardiovascular risk factors, and prevalent cardiovascular disease in men and women. The British Regional Heart Study. *Stroke* 1999; **30**: 841–850.
12 Prati P, Tosetto A, Vanuzzo D, Bader G, Casaroli M, Canciani L, Castellani S, Touboul PJ. Carotid intima media thickness and plaques can predict the occurrence of ischemic cerebrovascular events. *Stroke* 2008; **39**: 2470–2476.
13 Cupini LM, Pasqualetti P, Diomedi M, Vernieri F, Silvestrini M, Rizzato B, Ferrante F, Bernardi G. Carotid artery intima-media thickness and lacunar versus nonlacunar infarcts. *Stroke* 2002; **33**: 689–694.
14 de Leeuw FE, de Groot JC, Oudkerk M, Witteman JC, Hofman A, van Gijn J, Breteler MM. Aortic atherosclerosis at middle age predicts cerebral white matter lesions in the elderly. *Stroke* 2000; **31**: 425–429.
15 de Leeuw FE, de Groot JC, Bots ML, Witteman JC, Oudkerk M, Hofman A, van Gijn J, Breteler MMB. Carotid atherosclerosis and cerebral white matter lesions in a population based magnetic resonance imaging study. *J Neurol* 2000; **247**: 291–296.
16 Kelly R, Hayward C, Avolio A, O'Rourke M. Noninvasive determination of age-related changes in the human arterial pulse. *Circulation* 1989; **80**: 1652–1659.
17 Agabiti-Rosei E, Mancia G, O'Rourke MF, Roman MJ, Safar ME, Smulyan H, Wang JG, Wilkinson IB, Williams B, Vlachopoulos C. Central blood pressure measurements and antihypertensive therapy: a consensus document. *Hypertension* 2007; **50**: 154–160.
18 Tomita H, Kawamoto R, Tabara Y, Miki T, Kohara K. Blood pressure is the main determinant of the reflection wave in patients with type 2 diabetes. *Hypertension Res* 2008; **31**: 493–499.
19 Qureshi G, Brown R, Salciccioli L, Qureshi M, Rizvi S, Farhan S, Lazar J. Relationship between aortic atherosclerosis and non-invasive measures of arterial stiffness. *Atherosclerosis* 2007; **195**: e190–e194.
20 Nürnberger J, Keflioglu-Scheiber A, Opazo Saez AM, Wenzel RR, Philipp T, Schäfers RF. Augmentation index is associated with cardiovascular risk. *J Hypertens* 2002; **20**: 2407–2414.
21 Soga J, Nakamura S, Nishioka K, Umemura T, Jitsuiki D, Hidaka T, Teragawa H, Takemoto H, Goto C, Yoshizumi M, Chayama K, Higashi Y. Relationship between augmentation index and flow-mediated vasodilation in the brachial artery. *Hypertension Res* 2008; **31**: 1293–1298.
22 Handa N, Matsumoto M, Maeda H, Hougaku H, Ogawa S, Fukunaga R, Yoneda S, Kimura K, Kamada T. Ultrasonic evaluation of early carotid atherosclerosis. *Stroke* 1990; **21**: 1567–1572.
23 Handa N, Matsumoto M, Maeda H, Hougaku H, Kamada T. Ischemic stroke events and carotid atherosclerosis. Results of the Osaka Follow-up Study for Ultrasonographic Assessment of Carotid Atherosclerosis (the OSACA Study). *Stroke* 1995; **26**: 1781–1786.
24 Kohara K, Tabara Y, Oshiumi A, Miyawaki Y, Kobayashi T, Miki T. Radial augmentation index: a useful and easily obtainable parameter for vascular aging. *Am J Hypertens* 2005; **18**(suppl 1): S11–S14.
25 Fazekas F, Chawluk JB, Alavi A, Hurtig HI, Zimmerman RA. MR signal abnormalities at 1.5 T in Alzheimer's dementia and normal aging. *AJR Am J Roentgenol* 1987; **149**: 351–356.
26 Ginsberg MD, Hedley-Whyte ET, Richardson Jr EP. Hypoxic-ischemic leukoencephalopathy in man. *Arch Neurol* 1976; **33**: 5–14.
27 Paulson OB, Strandgaard S, Edvinsson L. Cerebral autoregulaion. *Cerebrovasc Brain Metab Rev* 1990; **2**: 161–192.
28 Pantoni L, Garcia JH. Pathogenesis of leukoaraiosis: a review. *Stroke* 1997; **28**: 652–659.
29 Roman MJ, Devereux RB, Kizer JR, Lee ET, Galloway JM, Ali T, Umans JG, Howard BV. Central pressure more strongly relates to vascular disease and outcome than does brachial pressure: the Strong Heart Study. *Hypertension* 2007; **50**: 197–203.
30 Pini R, Cavallini MC, Palmieri V, Marchionni N, Di Bari M, Devereux RB, Masotti G, Roman RJ. Central but not brachial blood pressure predicts cardiovascular events in an unselected geriatric population: the ICARe Dicomano Study. *J Am Coll Cardiol* 2008; **51**: 2432–2439.
31 Grassi G, Borghi C. Central blood pressure as estimate of cardiovascular risk: potentials and limitations. *J Hypertens* 2008; **26**: 16–17.
32 Sharman JE, Stowasser M, Fassett RG, Marwick TH, Franklin SS. Central blood pressure measurement may improve risk stratification. *J Hum Hypertens* 2008; **22**: 838–844.
33 Williams B, Lacy PS, Thom SM, Cruickshank K, Stanton A, Collier D, Hughes AD, Thurston H, O'Rourke M. Differential impact of blood pressure-lowering drugs on central aortic pressure and clinical outcomes: principal results of the Conduit Artery Function Evaluation (CAFE) study. *Circulation* 2006; **113**: 1213–1225.
34 Kim DH, Kim J, Kim JM, Lee AY. Increased brachial-ankle pulse wave velocity is independently associated with risk of cerebral ischemic small vessel disease in elderly hypertensive patients. *Clin Neurol Neurosurg* 2008; **110**: 599–604.
35 Ohmine T, Miwa Y, Yao H, Yuzuriha T, Takashima Y, Uchino A, Takahashi-Yanaga F, Morimoto S, Maehara Y, Sasaguri T. Association between arterial stiffness and cerebral white matter lesions in community-dwelling elderly subjects. *Hypertens Res* 2008; **31**: 75–81.
36 Fantini F, Mattocks A, Bulpitt CJ, Banya W, Rajkumar C. Is augmentation index a good measure of vascular stiffness in the elderly? *Age Ageing* 2007; **36**: 43–48.
37 Gatzka CD, Cameron JD, Dart AM, Berry KL, Kingwell BA, Dewar EM, Reid CM, Jennings GL. Correction of carotid augmentation index for heart rate in elderly essential hypertensives. ANBP2 Investigators. Australian Comparative Outcome Trial of Angiotensin-converting enzyme inhibitor and diuretic based treatment of hypertension in the elderly. *Am J Hypertens* 2001; **14**: 573–577.

Circ J 2009; **73:** 1945 – 1949

Diagonal Ear-Lobe Crease is Correlated With Atherosclerotic Changes in Carotid Arteries

Isha Shrestha, MD; Toshiho Ohtsuki, MD; Tetsuya Takahashi, MD;
Eiichi Nomura, MD*; Tatsuo Kohriyama, MD; Masayasu Matsumoto, MD

Background: The diagonal ear-lobe crease (ELC) is reported to be a marker of cardiovascular disease. Very few reports have assessed the relationship of ELC with atherosclerosis. This relationship is investigated here using a Japanese population.

Methods and Results: A prospective cross-sectional study included 212 consecutive patients. Bilateral ear lobes were checked for the ELC and this was followed by carotid ultrasonography to measure the far wall common carotid artery intima-media thickness (CCA-IMT), plaque score (PS) and plaque number (PN). Patients with ELC had significantly higher carotid IMT than controls (0.90±0.24 vs 0.77±0.15, respectively, P<0.001). ELC presence correlated significantly with carotid IMT, PS, and PN (r=0.306, P<0.0001; r=0.198, P<0.008 and r=0.221, P<0.0001, respectively), and also with age, male sex and hypertension. ELC presence and absence in mild or no PS and moderate or severe PS subgroups was significant, with a chi-squared value of 7.59 (P<0.006). In multivariate regression analysis, ELC presence correlated with CCA-IMT independently. The odds ratio for the presence of ELC in patients with CCA-IMT of <0.8 mm vs patients with CCA-IMT of ≥0.8 mm (the median value) was 0.41 (95% confidence interval, 0.22–0.76).

Conclusions: The present study showed an association between ELC and increased CCA-IMT, PS, and PN. (*Circ J* 2009; **73:** 1945 – 1949)

Key Words: Atherosclerosis; Carotid intima-media thickness; Diagonal ear-lobe crease; Plaque score

Ear-lobe crease (ELC) is the fold or crease in the skin of the ear-lobe, first described by Frank in 1973.[1] Since then, there have been many other reports about ELC as a risk factor for coronary artery disease (CAD). While many studies have been reported regarding the relationship of ELC with CAD, very few have been reported regarding the correlation with atherosclerosis of the carotid artery.[2,3] The carotid artery intima-media thickness (IMT) is not only taken as one of the risk factors for cerebrovascular disease (CVD), but it is also considered as a reliable marker of systemic atherosclerosis.[4–6] This study has been designed in this regard, to study the prevalence of the ELC in relation to the carotid atherosclerosis, and to find out whether it can be used as a marker of carotid atherosclerosis and thus an indicator of future stroke. In this study, we also investigated the association of ELC with other established risk factors for atherosclerosis (ie, hypertension, hyperglycemia, dyslipidemia and smoking habits).

Editorial p 1801

Methods

A continuous prospective cross-sectional study was conducted. Patients were recruited from consecutive cases undergoing clinically indicated ultrasonographic examination of the extracranial carotid artery systems, and included a wide age-group range and underlying diseases or diagnoses, including patients with CVD history, CAD history, patients with other neurological and systemic problems and also the patients undergoing carotid ultrasonography for pre-operative screening purposes, in the department of Neurology, Hiroshima University Hospital. Exclusion criteria included the inability to obtain a good carotid sonograph, and the inability to obtain informed consent from the patient. Informed consent was obtained from all the participants before they enrolled in the study.

The bilateral ear lobes were assessed manually for the presence of typical diagonal ELC, with the patients in sitting position using an evaluation sheet (**Figure 1**). The structure of the ear lobe, presence or absence of the ELC and if present, the length and depth of the crease were recorded on the sheet. An illustration of an ear lobe was also included on each sheet where the ELC was drawn exactly as present and later on tallied with a photograph of a typical ELC. The typical ELC was recorded as being present if a subject had a deep diagonal crease extending obliquely from the tragus towards the outer border of the ear lobe, covering at least two-thirds of the ear lobe length. Whenever there was more than 1 crease, at least 1 should have met the above criteria. A typical ELC in one of the patients is shown in **Figure 1**

(Received February 27, 2009; revised manuscript received May 15, 2009; accepted May 24, 2009; released online July 31, 2009)

Department of Clinical Neuroscience and Therapeutics, Hiroshima University Graduate School of Biomedical Sciences, *Department of Neurology, Suiseikai Kajikawa Hospital, Hiroshima, Japan

Mailing address: Tetsuya Takahashi, MD, Department of Clinical Neuroscience and Therapeutics, Hiroshima University Graduate School of Biomedical Sciences, 1-2-3 Kasumi, Minami-ku, Hiroshima 734-8551, Japan. E-mail: tetakaha@mac.com

All rights are reserved to the Japanese Circulation Society. For permissions, please e-mail: cj@j-circ.or.jp

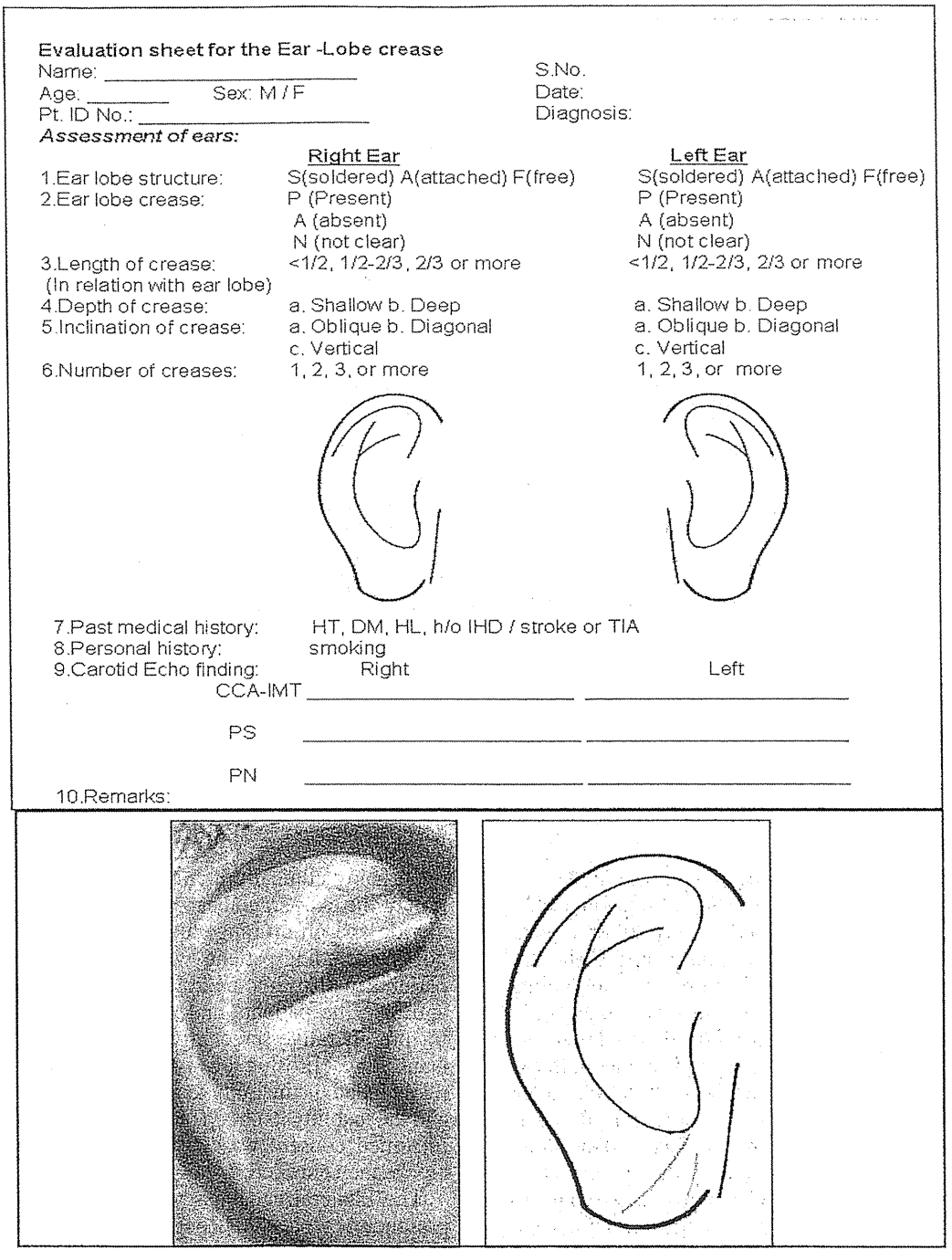

Figure 1. Ear-lobe crease evaluation sheet used in the study (**Above**). Ear with a typical ear-lobe crease and the marking of the same in the evaluation sheet illustration (**Below**).

as an example, along with the recording of the crease in the evaluation sheet illustration (**Figure 1**). To minimize the risk of examiner's bias, the ear lobes were evaluated prior to the ultrasonographic examination. The examiner conducting the ultrasonography was blinded to the patient ELC findings.

Common carotid arteries were evaluated with high resolution B-mode duplex ultrasonography with a 7.5 MHz linear type probe (Aplio, Toshiba Medicals, Tokyo, Japan). Bilateral optimal visualization of the carotid arteries was performed with the patients lying comfortably in the supine position with their neck slightly hyper-extended. The mean value of the maximal IMT measured in the distal common carotid artery (CCA) far wall (10 mm section of the artery proximal to the starting point of the carotid bulb) on the both sides was taken. IMT is the distance between the lumen-intima interface and the media-adventitia interface. Based on multiple visualizations, the measurements were taken from the best longitudinal images possible to obtain for the segment of the artery. The plaques in the accessible segments of the CCA as well as internal carotid arteries (ICA) were recorded in terms of plaque number (PN) and plaque score (PS). Plaques are defined as an IMT of ≥1.1 mm, and the PN includes the total number of plaques recorded in the CCA-ICA segments bilaterally. The PS is the sum of the heights of all the number of plaques present, bilaterally.[7,8]

Data regarding other established risk factors for atherosclerosis, namely hypertension, hyperglycemia, dyslipid-

Table. Characteristics of the Study Subjects

	All subjects (n=212)	ELC group (n=61)	No ELC group (n=151)	P value
Age (years)	67±12	72±8	65±13	0.001
Male (%)	102 (50)	42 (69)	64 (42)	0.0001
H/o stroke/TIA (%)	93 (46)	33 (54)	61 (40)	NS
H/o CAD/IHD (%)	24 (11)	5 (8)	19 (12)	NS
H/o PAD (%)	8 (4)	2 (3)	6 (4)	NS
Hypertension (%)	117 (55)	41 (67)	76 (50)	<0.05
Diabetes mellitus (%)	65 (31)	23 (37)	42 (27)	NS
Dyslipidemia (%)	77 (36)	20 (33)	57 (37)	NS
Smoking (%)	76 (36)	27 (44)	49 (32)	NS
SBP (mmHg)	135±22	141±25	132±21	0.001
DBP (mmHg)	77±12	76±13	77±12	NS
CCA max IMT (mm)	0.82±0.19	0.90±0.24	0.77±0.15	0.0001
Plaque score (PS)	3.61±3.59	5.72±3.84	4.21±2.73	0.001
Plaque number (PN)	2.34±2.39	3.83±2.50	2.53±1.61	0.001

Data are presented as mean±standard deviations or as the number (%) of patients.
ELC, ear-lobe crease; H/o, history of; TIA, transient ischemic attack; NS, not significant; CAD, coronary artery disease; IHD, ischemic heart disease; PAD, peripheral arterial disease; SBP, systolic blood pressure; DBP, diastolic blood pressure; CCA, common carotid artery; max, maximum; IMT, intima-media thickness.

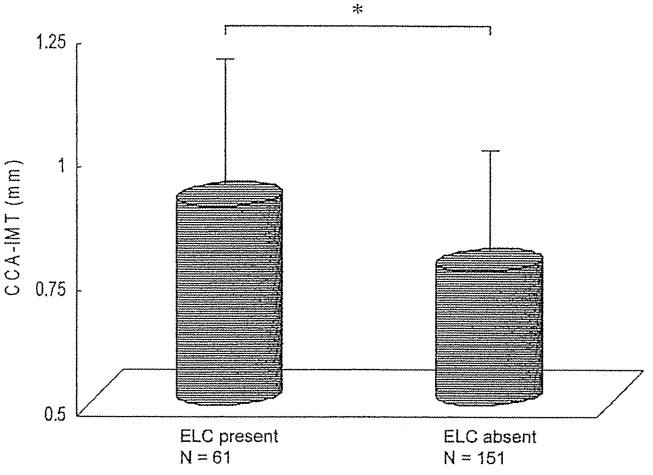

Figure 2. Common carotid artery intima-media thickness (CCA-IMT) in patients with and without ear-lobe crease (ELC). Data are presented as mean±standard deviation. P<0.0001.

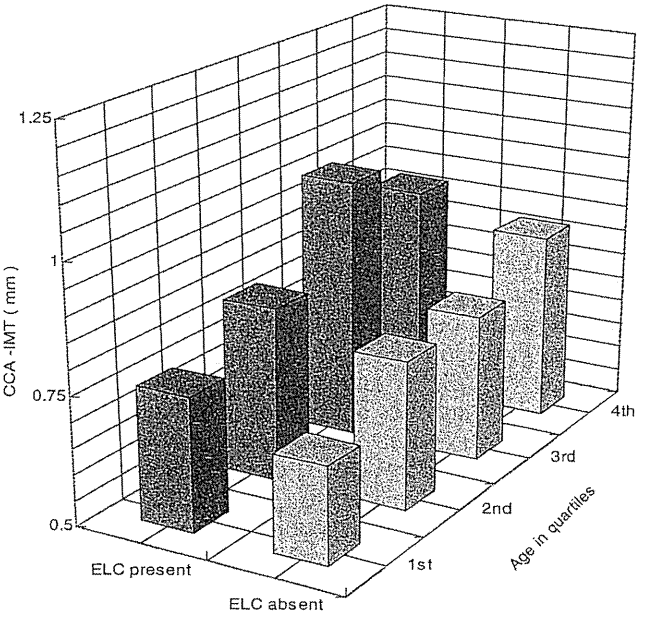

Figure 3. Common carotid artery intima-media thickness (CCA-IMT) in ear-lobe crease (ELC)-present and ELC-absent groups against quartiles of age.

emia, smoking habits and significant past medical illnesses such as transient ischemic attack (TIA)/stroke or ischemic heart disease (IHD)/CAD were drawn from hospital records. Risk factors were defined as follows: hypertension: SBP of ≥140 mmHg and/or DBP of ≥90 mmHg or using antihypertensive medication; hyperglycemia: fasting blood glucose of ≥7.0 mmol/L and/or glycosylated hemoglobin of ≥5.8% or using oral hypoglycemic agents or insulin; dyslipidemia: LDL-cholesterol of ≥3.6 mmol/L or using lipid lowering agents. Smoking was defined as "current smokers" or "non-smokers".

Statistical Analysis

Data were expressed as mean±standard deviation or % unless stated otherwise. P values of <0.05 were considered statistically significant. Comparison of the variables between groups was carried out using a chi-squared test for categorical variables and a t-test for continuous variables. Spearman and Pearson correlation analysis were performed to assess the relationship between ELC and other parameters. Multivariate regression analysis was conducted to check the independent relationship between ELC and carotid IMT. Cross tabulation and an odds ratio calculation was conducted to check the ELC in the 2 IMT groups. All statistical analysis was conducted using SPSS (Statistical Package for Social Sciences, release 11.0) for Windows.

Results

The study subjects consisted of 212 patients, 61 with typical ELC and 151 without ELC (as control group). Of the total 212, 106 (50%) were male. The mean age of the subjects was 67±12 years. The clinical characteristics of the study subjects are shown in **Table**. Of the total patients, 93 had a history of stroke or TIA, 24 had a history of CAD/IHD and 8 had peripheral vascular disease.

IMT was significantly higher in the ELC group than in the control group (0.90±0.24 vs 0.77±0.15, respectively, P<0.001) (**Figure 2**). The presence of ELC showed a significant correlation with carotid IMT (r=0.31, P<0.0001). The presence of ELC was also significantly correlated with

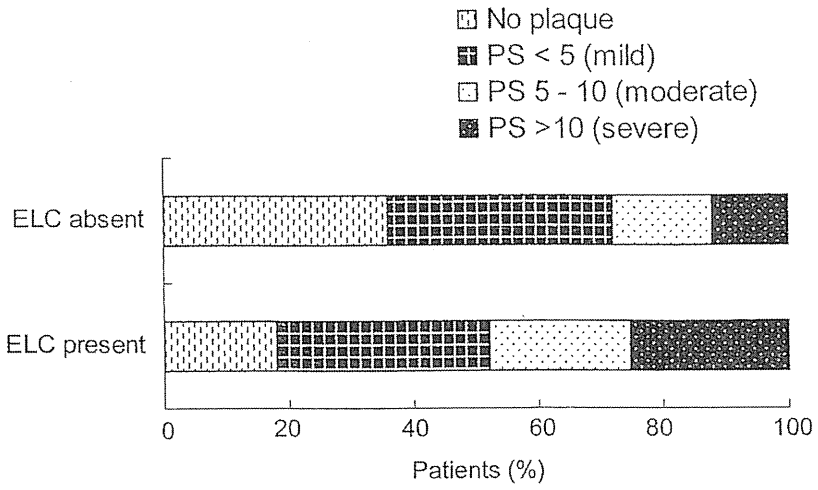

Figure 4. Atherosclerosis expressed as plaque score (PS) grades in patients with ear-lobe crease (ELC) and without ELC. PS <5=mild; PS 5–10=moderate and PS >10=severe.

age (r=0.24, P<0.001), male sex (r=0.24, P<0.0001) and presence of hypertension (r=0.15, P<0.05) but not with other risk factors, such as hyperglycemia, dyslipidemia and smoking habits.

The odds ratio for the presence of ELC in patients with CCA-IMT of <0.8 mm vs patients with CCA-IMT of ≥0.8 mm (the median value) was 0.41 (95% confidence interval, 0.22–0.76).

The subgroup analysis showed a graded and independent association of ELC and quartiles of age. The t-test analysis of the differences in the mean IMT in ELC-present and ELC-absent groups in different age quartiles showed significant differences between the 2 groups (0.72±0.02 vs 0.69±0.16 mm, P=0.036; 0.84±0.09 vs 0.78±0.13 mm, P<0.027; 0.96±0.34 vs 0.78±0.11 mm, P=0.008; respectively for the 1st, 2nd and 3rd quartiles but not for the 4th quartile (0.97±0.11 vs 0.91±0.15 mm, P=0.193, **Figure 3**)). ELC also showed an independent association with carotid IMT in the multivariate regression analysis (β=0.306, P≤0.0001) when adjusted for age, sex and hypertension.

Our results showed that the PS and PN were higher in ELC-present group compared to the control group. In the ELC-present group, almost 48% had modefate-to-severe atherosclerotic findings, whereas in the control group had only 27% moderate-to-severe atherosclerotic changes (**Figure 4**).

There was significant correlation between ELC and PS, as well as PN (r=0.198, P<0.008 and r=0.221, P<0.0001, respectively). Grading of atherosclerotic changes is conducted based on the PS, where a PS of <5 is considered as mild, 5–10 as moderate and >10 as severe.[8] PSs in the subjects were further divided into mild or no PS and moderate to severe PS sub groups, and compared between ELC-present and -absent groups. The chi-squared value for this analysis was 7.59 (P<0.006).

Discussion

The main finding of this study is that ELC is significantly associated with carotid artery IMT and also with the PS and PN, the markers of atherosclerotic changes in the arteries. Since the first reporting of ELC by Frank in 1973, many other studies about ELC as a risk factor for CAD have been reported.[1,9–19] While many studies have been reported regarding the relationship of ELC with CAD, very few have been reported on the correlation with atherosclerosis of the carotid artery.[2,3] Few have studied the correlation of ELC with carotid atherosclerosis, but they also have studied only the relationship with carotid IMT, not other indices of carotid artery ultrasonography such as PS and PN. Celik et al have reported a significant association between ELC and the carotid IMT in a population sample of middle-aged adults without known atherosclerotic disease.[3] In this regard, the present study also supports the association between ELC and carotid IMT. To the best of our knowledge, this is the first published report regarding the association between carotid IMT, carotid PS and ELC in an oriental population.

Studies in the past have examined the clinical and pathological correlations and found degeneration of elastin in the ELCs, tear in elastic fibers and pre-arteriolar wall thickening.[20,21] In contrast, atherosclerotic changes in the arterial wall could include smooth muscle cell proliferation, deposition of lipid and accumulation of collagen, elastin and proteoglycans, without the compensatory development of scar collagen. Changes in the ratio of collagen to elastin have been known to structurally affect the elastic behavior of the arterial wall.[22–24] This pathological mechanism might be the possible explanation for the correlation we found for the first time between the ELC and the atherosclerotic changes, especially the plaques in the carotid artery. Thus, in addition to the primary role of ageing and hypertension, some other atherogenic stimuli might be involved in the development of the ELC and also the atherosclerotic changes in the arteries.

Most studies in past agree that, although the prevalence of the ELC increases with advancing age, the correlation of the ELC with CAD is independent of this phenomenon,[10] however, some reports have tried to attribute the relationship between ELC and CAD as being solely dependent on age. On par with most of the past studies, we also found an increasing trend of ELC prevalence with increasing age, but the relationship of ELC with IMT was independent of age and sex. Tranchesi Jr et al have also reported a significant association between ELC and CAD in quite a large sample of patients (1,424 patients), irrespective of patient's chronological age and sex, however, they did find the growing prevalence of ELC with advancing age.[15] Many other investigators have also reported similar findings.[11,13,14,19,20,25] Studies have shown that ELC has a reasonably high predictive value for cardiac events.[15,26] Kirkhim et al and Elliot and Karrison have reported the association of ELC with an increased risk of cardiovascular cause of death.[16,17] Higuchi et al, in a recent study, demonstrated an association between

ELC and atherosclerotic cardiovascular disease in metabolic syndrome patients.[27] Various studies have found varying degrees of association between ELC and CAD, and various mechanisms of association are suggested. Systemic arterial atherosclerosis is a progressive condition and involves various arteries leading to some of the most devastating outcomes. Hoshino et al report that metabolic syndrome and intracranial large artery atherosclerosis might be potential predictors for identifying patients with cerebral infarction who are at the highest risk of asymptomatic CAD.[28] Li et al have demonstrated the importance of the detection of the vulnerable plaques.[29] These and many other studies highlight the importance of the simple and reliable predictors of atherosclerosis like ELC for the detection of the atherosclerotic changes as early as possible. Identification of the persons at risk of such major outcomes in the earlier stages would lower the burden of morbidities and mortalities associated with these disorders.

Agreeing with the previous studies, we also suggest that ELC should be promoted as a marker of possible atherosclerotic changes, and it might serve as a reminder to those patients who might not otherwise be screened for modifiable risk factors for atherosclerosis and also provide caution for possible future diagnosis of CAD or CVD. As ELC is a very easily detectable sign, it can be promoted as a simple index of carotid atherosclerosis, and therefore a simple predictor of a possible devastating consequence. It can easily be applied in any setting, even by primary level health-care professionals for the screening of the patients in terms of a future risk of stroke.

The present study had some limitations; small sample size, and having a cross-sectional study design. In conclusion, this study suggests that the presence of ELC might be considered as a possible sign of underlying atherosclerotic disease, although further studies are still required to establish it as a reliable (diagnostic) sign in clinical practice.

Acknowledgement

We thank Ms Akemi Enomura (Department of Clinical Neuroscience and Therapeutics, Hiroshima University) for conducting all the carotid ultrasonographies in the present study.

Disclosure

Financial disclosure and conflicts of interest: NO disclaimers.

References

1. Frank ST. Aural sign of coronary artery disease. *N Engl J Med* 1973; **289:** 327–328.
2. Kobayashi Y, Fukuo Y, Nakazawa Y, Kato H, Shibuya T, Terashi S, et al. The evaluation of the diagonal ear lobe crease (ELC) as an atherosclerotic sign. *Jpn J Geriat* 1987; **24:** 525–531 (in Japanese).
3. Celik S, Erdoan T, Gedikli O, Kiris A, Erem C. Diagonal ear-lobe crease is associated with carotid intima-media thickness in subjects free of clinical cardiovascular disease. *Atherosclerosis* 2007; **192:** 428–431.
4. Nagai Y, Matsumoto M, Metter EJ. The carotid artery as a noninvasive window for cardiovascular risk in apparently healthy individuals. *Ultrasound Med Biol* 2002; **28:** 1231–1238.
5. Roederrer GO, Langlois YE, Jager KA, Primozich JF, Beach KW, Phillips DJ, et al. The natural history of carotid arterial disease in asymptomatic patients with cervical bruits. *Stroke* 1984; **15:** 605–613.
6. Crouse JR, Toole JF, McKinney WM, Dignan MB, Howard G, Kahl FR, et al. Risk factors for extracranial carotid artery atherosclerosis. *Stroke* 1987; **18:** 990–996.
7. Handa N, Matsumoto M, Maeda H, Hougaku H, Kamada T. Ischemic stroke events and carotid atherosclerosis: Results of the Osaka follow-up Study for ultrasonographic Assessment of Carotid Atherosclerosis (the OSACA Study). *Stroke* 1995; **26:** 1781–1786.
8. Handa N, Matsumoto M, Maeda H, Hougaku H, Ogawa S, Fukunaga R, et al. Ultrasonic evaluation of early carotid atherosclerosis. *Stroke* 1990; **21:** 1567–1572.
9. Wagner RF Jr, Reinfeld HB, Wagner KD, Gambino AT, Falco TA, Sokol JA, et al. Ear canal hair and the ear lobe crease as predictors for coronary artery disease. *N Engl J Med* 1984; **311:** 1317–1318.
10. Elliott WJ. Ear lobe crease and coronary artery disease: 1000 patients and review of the literature. *Am J Med* 1983; **75:** 1024–1032.
11. Kaukola S, Manninen V, Valle M, Halonen PI. Ear-lobe crease and coronary atherosclerosis. *Lancet* 1979; **2:** 1377.
12. Moncada B, Ruiz JM, Rodriguez E, Leiva JL. Ear-lobe crease. *Lancet* 1979; **1:** 220–221.
13. Christiansen JS, Mathiesen B, Andersen AR, Calberg H. Letter: Diagonal ear lobe crease in coronary heart disease. *N Engl J Med* 1975; **293:** 308–309.
14. Lichstein E, Chadda KD, Naik D, Gupta PK. Diagonal ear-lobe crease: Prevalence and implications as a coronary risk factor. *N Engl J Med* 1974; **290:** 615–616.
15. Tranchesi B Jr, Barbosa V, de Albuquerque CP, Caramelli B, Gebara O, dos Santos Filho RD, et al. Diagonal ear lobe crease as a marker of the presence and extent of coronary atherosclerosis. *Am J Cardiol* 1992; **70:** 1417–1420.
16. Kirkham N, Murrells T, Melcher DH, Morrison EA. Diagonal earlobe creases and fatal cardiovascular disease: A necropsy study. *Br Heart J* 1989; **61:** 361–364.
17. Elliott WJ, Karrison T. Increased all-cause and cardiac morbidity and mortality associated with the diagonal earlobe crease: A prospective cohort study. *Am J Med* 1991; **91:** 247–254.
18. Rhoads GG, Yano K. The ear lobe crease and coronary artery heart disease. *Ann Intern Med* 1977; **87:** 245.
19. Elliott WJ, Powell LH. Diagonal earlobe creases and prognosis in patients with suspected coronary artery disease. *Am J Med* 1996; **100:** 205–211.
20. Shoenfeld Y, Mor R, Weinberger A, Avidor I, Pinkhas J. Diagonal ear lobe crease and coronary risk factors. *J Am Geriatr Soc* 1980; **28:** 184–187.
21. Wermut W, Jaszczenko S, Ruszel A. Ear lobe crease as a risk factor in coronary disease. *Wiad Lek* 1980; **33:** 435–438 (in Polish).
22. Riley WA, Evans GW, Sharrett AR, Burke GL, Barnes RW. Variation of common carotid artery elasticity with intimal-medial thickness: The ARIC Study: Atherosclerosis Risk in Communities. *Ultrasound Med Biol* 1997; **23:** 157–164.
23. Stary HC. Evolution and progression of atherosclerotic lesions in coronary arteries of children and young adults. *Arteriosclerosis* 1989; **9**(1 Suppl): I-19–I-32.
24. Zureik M, Temmar M, Adamopoulos C, Bureau JM, Courbon D, Thomas F, et al. Carotid plaques, but not common carotid intima-media thickness, are independently associated with aortic stiffness. *J Hypertens* 2002; **20:** 85–93.
25. Miric D, Fabijanic D, Giunio L, Eterovic D, Culic V, Bozic I, et al. Dermatological indicators of coronary risk: A case-control study. *Int J Cardiol* 1998; **67:** 251–255.
26. Nyboe J, Jensen G, Appleyard M, Schnohr P. Risk factors for acute myocardial infarction in Copenhagen City heart study. *Eur Heart J* 1989; **10:** 910–916.
27. Higuchi Y, Maeda T, Guan JZ, Oyama J, Sugano M, Makino N. Diagonal earlobe crease are associated with shorter telomere in male Japanese patients with metabolic syndrome. *Circ J* 2009; **73:** 274–279.
28. Hoshino A, Nakamura T, Enomoto S, Kawahito H, Kurata H, Nakahara Y, et al. Prevalence of coronary artery disease in Japanese patients with cerebral infarction: Impact of metabolic syndrome and intracranial large artery atherosclerosis. *Circ J* 2008; **72:** 404–408.
29. Li ZY, Tang T, U-King-Im J, Graves M, Sutcliffe M, Gillard JH. Assessment of carotid plaque vulnerability using structural and geometrical determinants. *Circ J* 2008; **72:** 1092–1099.

Cerebrovasc Dis 2009;27:616–617
DOI: 10.1159/000218073

Advantages of High b Value Diffusion-Weighted Imaging in the Diagnosis of Acute Stroke – A Case Report

Aidos Doskaliyev [a], *Fumiyuki Yamasaki* [a], *Taiichi Saito* [a], *Eiichi Nomura* [b], *Kazuhiko Sugiyama* [a], *Toshiho Ohtsuki* [b], *Masayasu Matsumoto* [b], *Kaoru Kurisu* [a]

Departments of [a] Neurosurgery and [b] Clinical Neuroscience and Therapeutics, Graduate School of Biomedical Sciences, Hiroshima University, Hiroshima, Japan

Introduction

It may be possible to use the mismatch in perfusion- and diffusion-weighted images (PWI, DWI) on scans acquired within 6 h of symptom onset to identify salvageable tissues in patients with acute ischemic stroke [1]. Although it has been shown that DWI is sensitive for the diagnosis of acute ischemic lesions, there is increasing evidence that in some situations it may initially fail to detect acute lesions. We show that DWI obtained with a high b value may represent a useful diagnostic tool for the rapid and accurate identification of acute ischemic brain infarctions.

Case Report

A 73-year-old man with acute-onset dizziness and ataxia was admitted to Hiroshima University Hospital. MR angiography (MRA) performed within 6 h of symptom onset showed that the left superior cerebellar artery was occluded (fig. 1a), although DWI based on b value of 1,000 s/mm^2 ($DWI_{1,000}$) failed to identify any obvious changes in the cerebellum (fig. 1b). On the other hand, on DWI based on a b value of 4,000 s/mm^2 ($DWI_{4,000}$), there was an obvious high-intensity area in the upper left cerebellum supplied by the superior cerebellar artery (fig. 1c).

We administered anticoagulant therapy. A MRI study performed on the 8th day post-onset (fig. 1d) showed cerebellar lesions that were closely associated with the high-intensity lesion noted on the initial $DWI_{4,000}$. MRA revealed recanalization of the superior cerebellar artery.

Discussion

Early and accurate detection of acute ischemic stroke is required for treatment success and achieving improved quality of life for survivors. DWI detected infarcted tissue within 1 h of the insult in rats [2]. In clinical studies, DWI was 93–100% sensitive for the detection of stroke if the scans were acquired within 6 h of symptom onset [3, 4]. According to Lam et al. [5] up to 12.5% of hyperacute ischemic stroke was missed on the initial DWI scan. Some researchers [6, 7] have argued that a high b value at DWI does not confer a diagnostic advantage. We suspect that these

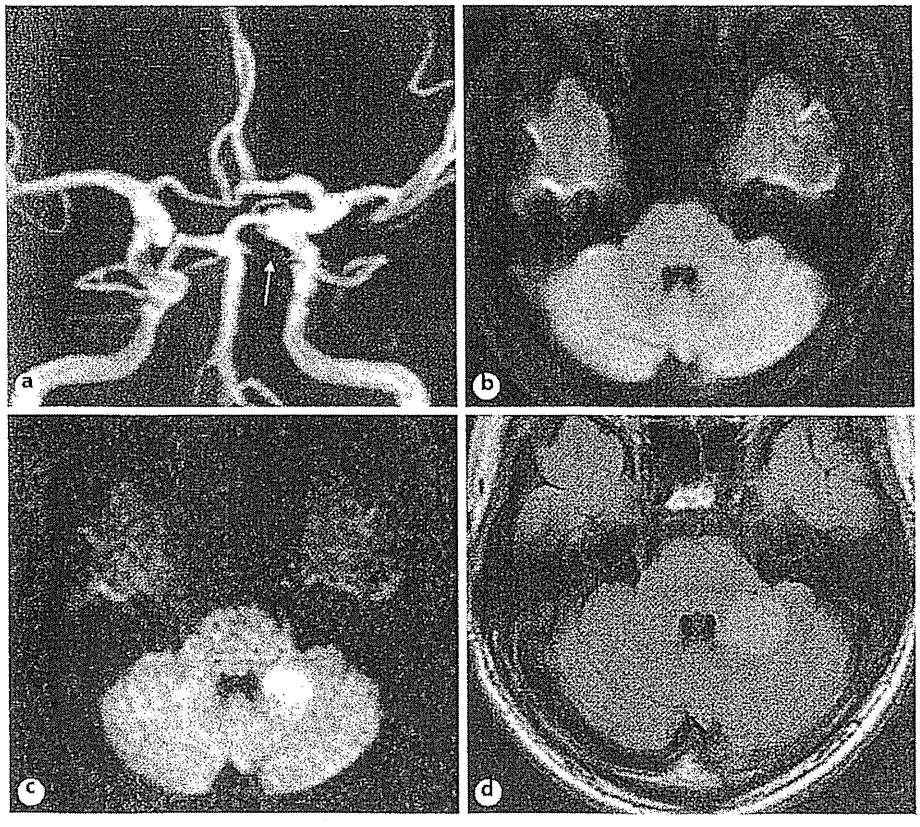

Fig. 1. All radiological examinations were performed on a 3-T MR scanner (Signa Excite HD 3.0T; GE Medical Systems, Milwaukee, Wisc., USA); the effective gradient was 40 mT/m, the slew rate was 150 mT/m/ms. The parameters of b = 1,000 and b = 4,000 DWI were: 8-channel phased array head coil, TR, 5,000 ms and TE, 66.2 ms (b = 1,000) and TR, 5,000 ms and TE, 96.4 ms (b = 4,000), NEX, 1; field of view (FOV), 220; slice thickness, 6 mm; gap, 1.0 mm; number of slices, 20; data acquisition matrix 128 × 128, and scan time, 20 and 40 s for b = 1,000 and b = 4,000, respectively. Images obtained within 6 h of symptom onset (**a**, **b**, **c**). MRA (**a**) shows occlusion of the left superior cerebellar artery (arrow). No ischemic lesions are evident on diffusion-weighted axial MR image (b value 1,000 s/mm^2) (**b**). However, the image acquired with a b value of 4,000 s/mm^2 (**c**) clearly shows an ischemic lesion in the cerebellum as an area of high signal intensity. FLAIR axial (**d**) MR images obtained 8 days after symptom onset show clear ischemic lesion in the cerebellum.

findings were acquired on 1.5-T scanners and that this entails some limitations. High b-value DWI requires a hardware upgrade because most scanners cannot generate a 40-mT/m gradient field [6]. Despite the lower MR signal intensity and lower signal-to-noise ratio on high b-value images [8], 3-T DWI is at least as good as, and in some ways superior to, 1.5-T DWI for assessing hyperacute stroke [9].

We postulate that one reason for missed acute ischemic stroke might be the conspicuity of acute ischemic lesions on diffusion-weighted images, which is related to the b-value. In some cases (as in this one) higher b-values might offer an opportunity for earlier lesion detection. We found that $DWI_{4,000}$ performed on the 3-T scanner was superior for the identification of ischemic lesions. Our findings suggest that the PWI-DWI mismatch time window is shorter than was previously thought. Studies are underway in our laboratory to determine the optimal b value for the assessment of acute stroke. Based on our findings, we suggest that high b-value DWI is useful for the selection of thrombolytic therapy in patients with acute stroke.

References

1 Kane I, Sandercock P, Wardlaw J: Magnetic resonance perfusion diffusion mismatch and thrombolysis in acute ischemic stroke: a systematic review of the evidence to date. J Neurol Neurosurg Psychiatry 2007;78:485–491.
2 Mintorovitch J, Moseley M, Chileuitt L, et al: Comparison of diffusion and T_2-weighted MRI for the early detection of cerebral ischemia and reperfusion in rats. Magn Reson Med 1991;18:39–50.
3 Gonzalez R, Schaefer P, Buonanno F, et al: Diffusion-weighted MR imaging: diagnostic accuracy in patients imaged within 6 hours of stroke symptom onset. Radiology 1999;210:155–162.
4 Saur D, Kuchinski T, Grzyska U, et al: Sensitivity and interrater agreement of CT and diffusion-weighted MR imaging in hyperacute stroke. AJNR Am J Neuroradiol 2003;24:878–885.
5 Lam WW, Wong KS, Rainer TH, et al: Assessment of hyperacute stroke like symptoms by diffusion-weighted images. Clin Imaging 2005;29:6–9.
6 Meyer J, Gutierrez A, Mock B, et al: High b-value diffusion-weighted MR imaging of suspected brain infarction. AJNR Am J Neuroradiol 2000;21:1821–1829.
7 Burdette J, Elster A: Diffusion-weighted imaging of cerebral infarctions: are higher b-values better? J Comput Assist Tomogr 2002;26:622–627.
8 Cihangiroglu M, Uluğ AM, Firat Z, et al: High b-value diffusion-weighted MR imaging of normal brain at 3 T. Eur J Radiol 2007.
9 Kosior RK, Wright CJ, Kosior JC: 3-Tesla versus 1.5-Tesla magnetic resonance diffusion and perfusion imaging in hyperacute ischemic stroke. Cerebrovasc Dis 2007;24:361–368.

Kaoru Kurisu, MD, PhD
Department of Neurosurgery
Graduate School of Biomedical Sciences
Hiroshima University
1-2-3 Kasumi, Minami-ku, Hiroshima, 734-8551 (Japan)
Tel. +81 82 257 5225, Fax +81 82 257 5229
E-Mail kuka422@hiroshima-u.ac.jp

Cerebrovasc Dis 2009;27:617–618
DOI: 10.1159/000218074

Large Carotid Thrombus

M.G. Delgado[a], P. Vega[b], V. Mateos[a], J. Bogousslavsky[c]

Departments of [a]Neurology and [b]Radiology, Hospital Central de Asturias, Oviedo, Spain; [c]Department of Neurology, Genolier Swiss Medical Network, Valmont-Genolier, Glion-sur-Montreux, Switzerland

A 76-year-old female with high blood pressure and atrial fibrillation as cerebrovascular risk factors was admitted because of sudden left hemiparesis and disarthria with a right periorbital headache. Transcranial Doppler ultrasound showed increased velocity in the right carotid siphon. Her cranial CT was normal. She was anticoagulated because of carotid siphon stenosis with low-molecular-weight heparin (0.6 ml subcutaneous nadroparin calcium every 12 h). An angio-CT showed calcified plaque in the right carotid siphon with a large thrombus (fig. 1A, B), resulting in a high-grade stenosis. We suggested the thrombus formation was due to a cardiac embolus stopped in the right

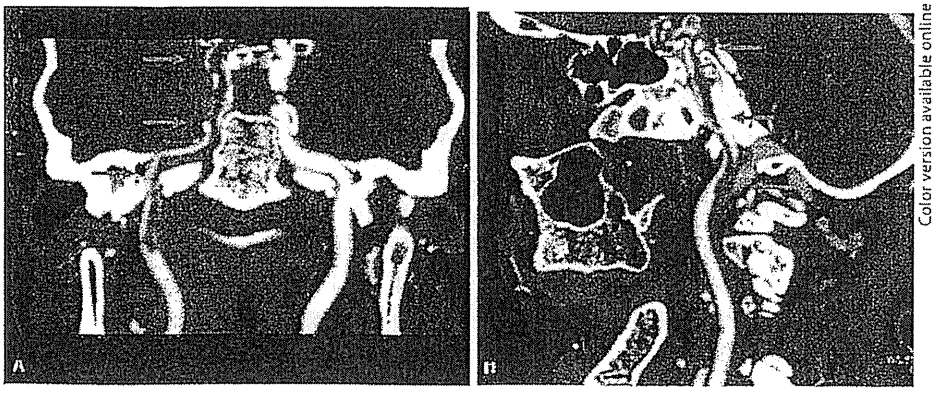

Color version available online

Fig. 1. Intra- and extracranial angio-CT. Coronal and lateral projections showed a large thrombus in the right internal carotid artery (arrows, red in the online version).